Pathology International

Pathology International 2011; **61**: 202–209 doi:10.1111/j.1440-1827.2011.02645.x

Original Article

Hypertension is positively associated with prostate cancer development in the TRAP transgenic rat model

Kentaro Takeshita, Satoru Takahashi, Mingxi Tang,* Azman Seeni,† Makoto Asamoto and Tomoyuki Shirai

Department of Experimental Pathology and Tumor Biology, Nagoya City University Graduate School of Medical Sciences, Nagoya, Japan

Epidemiological data on the relationship between hypertension and prostate cancer development are conflicting. To cast light on this question, we performed animal experiments using hybrid rats generated by crossing the spontaneously hypertensive rat (SHR) or its normotensive control Wistar Kyoto (WKY) rat with a transgenic rat for adenocarcinoma of prostate (TRAP) that features development of adenocarcinoma at high incidence by 15 weeks of age. The number of adenocarcinomatous foci in the lateral prostate of hypertensive (TRAP × SHR)F1 rats was demonstrated to be significantly increased compared with those of normotensive (TRAP × WKY)F1 rats. In the ventral prostate, increase of carcinoma foci was also observed but did not reach significance. The number of cancer foci showing microinvasion in (TRAP × SHR)F1 rats was higher than that of (TRAP × WKY)F1 rats, but again without significance, while treatment with prazosin, an anti-hypertensive agent, tended to decrease microinvasive carcinoma foci in both the ventral and lateral prostate. In conclusion, the present study provided additional evidence that high blood pressure is associated with prostate cancer risk.

Key words: hypertension, prazosin, prostate cancer, SHR, TRAP, WKY

Prostate cancer now has the highest incidence of all non-cutaneous neoplasms in men in Western countries such as Europe and the United States.[1] The prevalence of prostate cancer has also been increasing in Japan,[2] concomitantly with change in life-style. Epidemiologic and genomic studies have provided a great number of information concerning exogenous factors including diet, and environmental agents, as well as endogenous factors such as genetic predisposition for susceptibility, associated with the risk of prostate cancer.[3–5] Dietary factors, particularly fat or well-done meat intake, are considered to strongly contribute in the genesis of prostate cancer[6–8] partly on the evidence that Japanese immigrants to the United States showed an increased risk of prostate cancer.[9,10] Our previous studies demonstrated that 2-amino-1-methyl-6-phenylimidazo[4,5-b]pyridine (PhIP), one of the heterocyclic amines which are mutagenic compounds found in cooked meats, exerts carcinogenicity in the prostate, mammary gland and colon in rats,[11,12] and that spontaneously hypertensive rat (SHR) showed high susceptibility in PhIP-induced prostate carcinogenesis among the various strains of rats.[13] These findings prompted us to investigate the relationship between hypertension and prostate cancer development. To our knowledge, this is the first study of the effects of high blood pressure on prostate carcinogenesis in an *in vivo* animal model.

MATERIALS AND METHODS

Chemicals and animals

Prazosin hydrochloride, an α1-adrenergic receptor antagonist, was purchased from Sigma (St. Louis, MO, USA). Homozygous transgenic rat for adenocarcinoma of prostate (TRAP) with a Sprague-Dawley genetic background, which were established our laboratory,[14,15] were bred in our animal facility. Male F344 (F344/DuCrj) rats, male SHR (SHR/NCrj) rats, and male offspring from mating of the two strains were obtained from Charles River Japan (Yokohama, Japan). Male SHR/Izm and male normotensive

Correspondence: Satoru Takahashi, MD, PhD, Department of Experimental Pathology and Tumor Biology, Nagoya City University Graduate School of Medical Sciences, 1 Kawasumi, Mizuho-cho, Mizuho-ku, Nagoya 467-8601, Japan.
Email: sattak@med.nagoya-cu.ac.jp
Present address: *Department of Pathology, Luzhou Medical College, 319 ZhongShan road, Luzhou, Sichuan, China.
†School of Dental Sciences, Universiti Sains Malaysia, 16150 Kubang Kerian, Kelantan, Malaysia.
Received 14 July 2010. Accepted for publication 4 December 2010.

Wistar-Kyoto (WKY) (WKY/Izm) rats were from Japan SLC Inc. (Hamamatsu, Japan). They were housed 2–3/cage on wood-chip bedding in an air-conditioned animal room at 23 ± 2°C and 50 ± 10% humidity. Food and tap water were available *ad libitum*.

Experimental protocol

Experiment 1: Male F344 rats (n = 5), male SHR/NCrj rats (n = 5), male (F344 × SHR)F1 (n = 10) and male (SHR × F344)F1 rats (n = 10) were killed at 10 weeks of age and their prostate glands were removed and fixed in 10% neutral formalin.

Experiment 2: Homozygous female TRAP rats were mated with male SHR/Izm or male WKY/Izm rats to generate offspring. Eighteen male (TRAP × SHR/Izm)F1 and 18 male (TRAP × WKY/Izm)F1 offspring were randomly divided into two groups each, and designated as groups 1–4, respectively. Rats of groups 2 and 4 continuously received 2 mg/kg/day prazosin hydrochloride in drinking water starting at 10-weeks-old for 15 weeks while groups 1 and 3 served as controls receiving tap water alone. The systolic blood pressure of all rats was measured every week by tail-cuff plethysmography (KN-210, Natsume Seisakusho, Tokyo, Japan). The experiment was terminated when the animals were 25-weeks-old. Prostate glands were removed and fixed in formalin.

The present experiments were performed under protocols approved by the Institutional Animal Care and Use Committee of Nagoya City University Graduate School of Medical Sciences.

Assessment of epithelial hyperplasia in the ventral prostate

We calculated the percentage area occupied by epithelial cells in acini to determine hyperplastic changes in ventral prostate. Quantitative measurement was with an Image Processor for Analytical Pathology (IPAP, Sumika Technos Co., Osaka, Japan).

Evaluation of prostate neoplastic lesion development

Neoplastic lesions in prostate glands of TRAP rats were evaluated as previously described.[16] Briefly, neoplastic lesions were classified into three types, low-grade prostatic intraepithelial neoplasia (LG-PIN), high-grade PIN (HG-PIN) and adenocarcinoma, according to their structural morphologies. Low-grade PINs were characterized by having one or two layers of atypical cells with hyperchromatic nuclei and intact gland profiles. High grade PINs showed increased epithelial stratification, papillary or micropapillary proliferation of atypical epithelial cells but not filling in the acini with proliferative lesions. Adenocarcinomas were characterized by atypical cells filling almost all of the lumen of the ducts with cribriform structures or solid growth in acini (Fig. 1). The relative numbers of acini with the respective histological

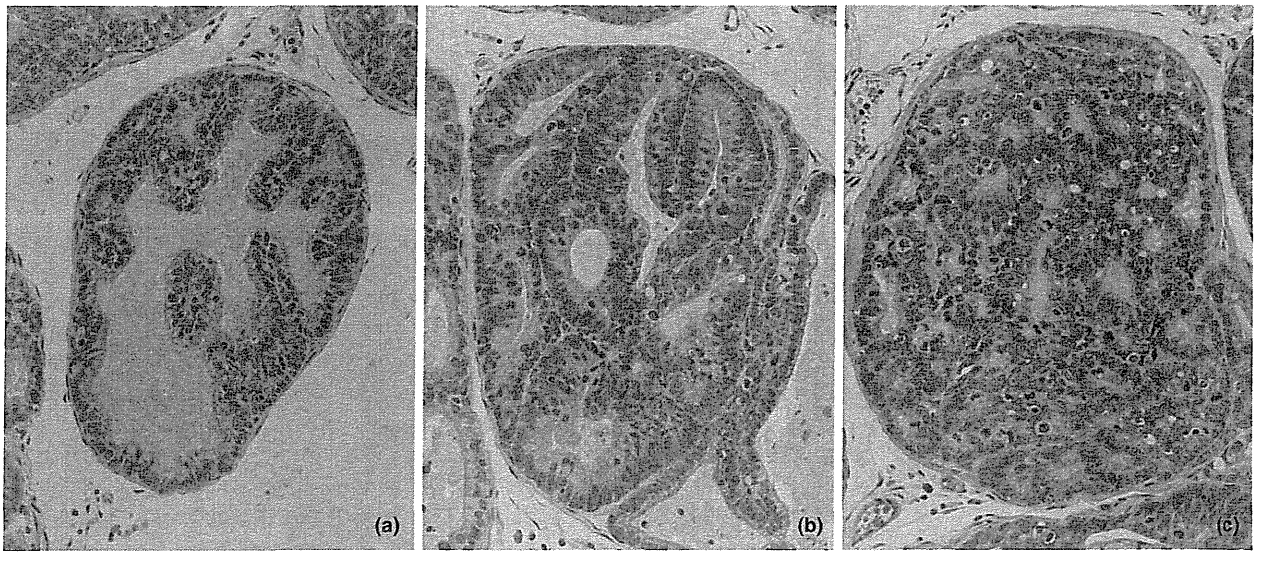

Figure 1 Representative histopathological findings for (**a**) low grade prostatic intraepithelial neoplasia (LG-PIN), (**b**) high grade PIN (HG-PIN) and (**c**) adenocarcinoma in lateral prostates of (spontaneously hypertensive rat (SHR) × TRAP)F1 rats.

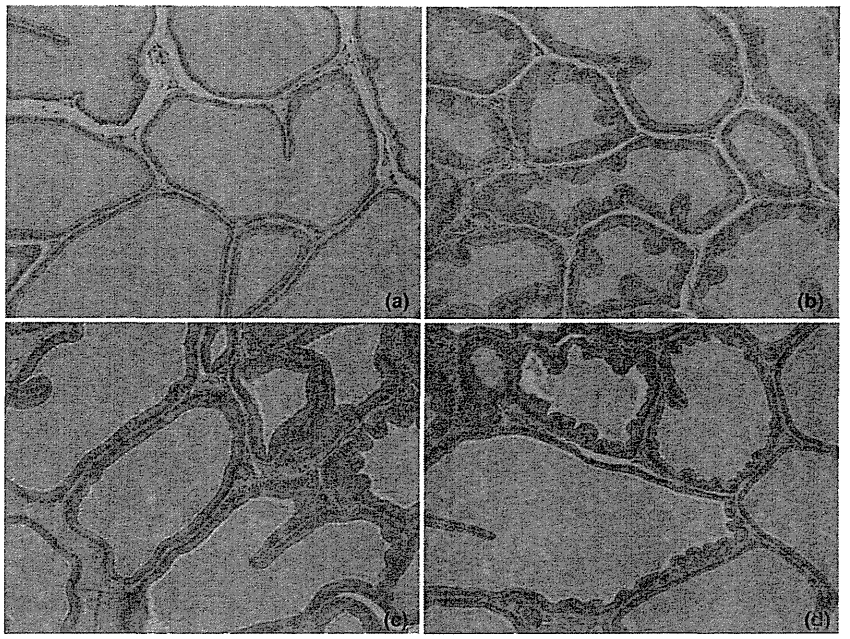

Figure 2 Representative histopathological findings for ventral prostates of (**a**) F344, (**b**) spontaneously hypertensive rat (SHR), (**c**) (F344 × SHR)F1 and (**d**) (SHR × F344)F1 rats.

characteristics were quantified by counting for the total acini in each prostatic lobe.

Immunohistochemistry

For Ki-67 immunostaining, deparaffinized sections were incubated with diluted rabbit polyclonal Ki-67 antibodies (Novocastra, Newcastle, UK). Apoptotic cells were detected using an In situ Apoptosis Detection Kit (terminal deoxynucleotidyl transferase-mediated dUTP nick end labeling (TUNEL) method) according to the manufacturer's instructions (Takara Bio Co. Ltd, Otsu, Japan). Labeling indices were counted separately in the ventral, dorsal and lateral prostate and expressed as numbers of Ki-67-positive or TUNEL-positive cells per 100 cells.

Statistical analysis

Differences in means between groups were determined by analysis of variance (ANOVA), followed by the Dunnett's post-hoc test with GraphPad Prism (version 5.0c) (GraphPad Software, Inc., La Jolla, CA, USA).

RESULTS

Experiment 1

As shown in Fig. 2, both (F344 × SHR)F1 and (SHR × F344)F1 offspring developed epithelial hyperplasia of the ventral prostate as reported previously for SHR rats.[17] Quantitative analysis revealed that degrees of lesion development in offspring were intermediate between those of parental F344 and SHR rats (Table 1). Values for (F344 × SHR)F1 were significantly higher than for their (SHR × F344)F1 counterparts.

Table 1 Quantitative data for epithelial content in ventral prostate of F344, SHR, and their F1 rats

Strain	No. of rats	Ventral prostate epithelium / acinus (%)
F344/DuCrj	5	28.8 ± 4.6
SHR/NCrj	5	51.4 ± 3.8
(F344 × SHR)F1	10	39.2 ± 4.7
(SHR × F344)F1	10	33.4 ± 5.9

$^{*}P < 0.05$, $^{**}P < 0.001$.
SHR, spontaneously hypertensive rat.

Experiment 2

Based on the results of Experiment 1, we generated hybrid rats of female TRAP rats mated with male SHR rats, or with normotensive control male WKY rats, to investigate the effect of hypertension on prostate carcinogenesis. Systolic blood pressure was sequentially monitored and the dose of prazosin was gradually increased up to 5 mg/kg/day as indicated in Fig. 3 because doses of 2 or 3 mg/kg/day proved ineffective. One rat from each of groups 2 and 4 were found dead

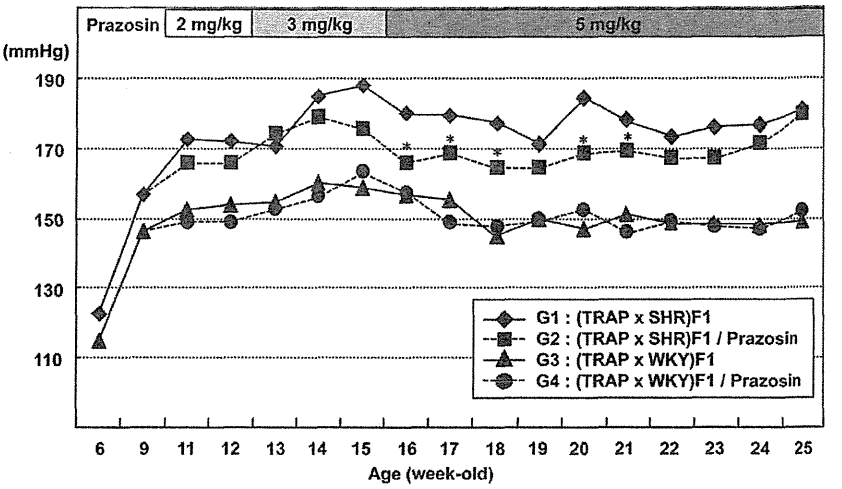

Figure 3 Sequential changes of systolic blood pressure in rats given prazosin. *$P <$ 0.05 vs. G1.

Table 2 Weights of final body, ventral prostate, and serum testosterone levels

Group	Treatment	No. of rats	Body weight (g)	Ventral prostate weight (g)	Serum testosterone (ng/mL)
1	(TRAP × SHR)F1	9	449.2 ± 17.9	0.31 ± 0.03	1.02 ± 0.28
2	(TRAP × SHR)F1 / Prazosin	8	434.9 ± 19.8	0.31 ± 0.04	2.64 ± 1.73*
3	(TRAP × WKY)F1	9	450.4 ± 18.6	0.33 ± 0.03	2.12 ± 1.18
4	(TRAP × WKY)F1 / Prazosin	8	441.9 ± 22.6	0.34 ± 0.05	1.07 ± 0.53

*$P < 0.05$ vs. Group 1.
TRAP, transgenic rat for adenocarcinoma of prostate; SHR, spontaneously hypertensive rat; WKY, Wistar Kyoto.

during the experiment from unknown causes. The final body weights of rats given prazosin tended to be lower than those of each non-treated control but the differences were not significant. Ventral prostate weights were almost the same among the groups. Effects of prazosin or hypertensive genetic background of SHR were variable on serum testosterone levels, but the values in group 2 were significantly higher than those of group 1 (Table 2).

All rats in the present study harbored adenocarcinoma foci in their prostates regardless of their size. The numbers in the lateral prostates of hypertensive (TRAP × SHR)F1 rats demonstrated a 78% significant increase compared with those of normotensive (TRAP × WKY)F1 rats (Table 3). In the ventral prostate, increase of carcinoma foci was also apparent in (TRAP × SHR)F1 but it did not reach statistical significance. Moreover, the proportions of preneoplastic and neoplastic lesions in the lateral prostate showed that prazosin treatment tended to suppress adenocarcinoma development about 31% in (TRAP × SHR)F1 rats (Table 3). We next focused on the effect of high blood pressure on microinvasive adenocarcinoma development which is age-dependent in our TRAP rats.[15] In the present study, the multiplicity of invasive carcinoma foci in (TRAP × SHR)F1 rats was greater, albeit without significance, than in (TRAP × WKY)F1 rats and a tendency for decrease was found in (TRAP × SHR)F1 rats given prazosin in both of the ventral and lateral prostate (Table 4). No differences in Ki-67 and apoptotic indices were found in any lobe among the groups (Fig. 4).

DISCUSSION

The present experiments provided evidence that prostate cancer risk in (TRAP × SHR)F1 offspring with high blood pressure was significantly higher than that in (TRAP × WKY)F1 rats. Although the anti-hypertensive effects of prazosin were somewhat weak there appeared to be some reduction in the incidence of adenocarcinomas. Since invasive lesions are observed after 35 weeks of age in TRAP rats,[15] it is plausible that associations would become more apparent by extension of the experimental period.

To date, conflicting results have been published regarding possible relationships between hypertension and the risk of prostate cancer. Clear links were reported in a population-based cohort study of 82 098 men in Norway[18] and a case-control study of 498 African-American men in the United States.[19] On the other hand, data from cohort studies in Sweden with 336 159 individuals and the United States with 58 704 men demonstrated no obvious connection.[20,21] With data concerning anti-hypertensive drugs, use of alpha-blockers, beta-blockers or angiotensin-I-converting enzyme (ACE) inhibitors may reduce prostate cancer risk[22–24] although

Table 3 Quantitative evaluation of neoplastic lesions in rat prostate

Group	Treatment	No. of rats	Relative number of acini with histological characteristics (%)									
			Ventral					Lateral				
			LG-PIN	HG-PIN	Adenocarcinoma			LG-PIN	HG-PIN	Adenocarcinoma		
					Non-invasive	Invasive	Total			Non-invasive	Invasive	Total
1	(TRAP × SHR)F1	9	25.6 ± 8.0	57.6 ± 8.8	16.7 ± 6.6	0.2 ± 0.3	16.9 ± 6.7	16.4 ± 5.1	69.1 ± 8.3	14.5 ± 6.3	0.2 ± 0.6	14.6 ± 6.6*
2	(TRAP × SHR)F1 / Prazosin	8	22.2 ± 5.2	62.0 ± 7.0	15.6 ± 9.1	0.2 ± 0.3	15.8 ± 9.2	20.6 ± 11.2	69.4 ± 13.3	9.8 ± 5.6	0.2 ± 0.4	10.0 ± 5.9
3	(TRAP × WKY)F1	9	26.6 ± 7.3	61.7 ± 8.0	11.6 ± 2.4	0.1 ± 0.2	11.7 ± 2.5	21.0 ± 8.7	70.7 ± 9.2	8.2 ± 5.2	0.1 ± 0.2	8.2 ± 5.0
4	(TRAP × WKY)F1 / Prazosin	8	26.8 ± 8.8	61.8 ± 10.0	11.4 ± 4.0	0	11.4 ± 4.0	14.0 ± 3.5	79.4 ± 5.2	6.5 ± 4.1	0.1 ± 0.3	6.6 ± 4.1

*$P < 0.05$ vs. Group 3.

LG-PIN, low grade prostatic intraepithelial neoplasia; HG, high grade; TRAP, transgenic rat for adenocarcinoma of prostate; SHR, spontaneously hypertensive rat; WKY, Wistar Kyoto.

prospective cohort studies provided no evidence that such medications exerted appreciable protective effects.[25,26]

One complicating factor might be gender and several reports have discussed the relationship between sex hormones and hypertension. Blood pressure in males is higher than in female SHR rats,[27] and young male SHR rats aged 9–10 weeks with chemical castration by flutamide treatment demonstrate delayed development of hypertension.[28,29] Moreover, administration of testosterone to ovariectomized female SHR rats exacerbates the disease.[30,31] There is thus mounting evidence that testosterone might play a promoting role in these animals. Intact (TRAP × SHR)F1 rats, however, showed the lowest level of serum testosterone among the groups and there was no clear association between testosterone levels and hypertension in the present study. Therefore, some factor(s) other than testosterone might be involved in the observed increased risk of prostate cancer development. A possible candidate factor is a genetic polymorphism of the angiotensin-converting enzyme (ACE) gene because this is reported to correlate with serum ACE levels,[32] blood pressure,[33] and the risk of prostate cancer in rats[34–36] and humans.[37,38] Prazosin is reported to not directly affect the renin-angiotensin system in terms of hypertension while inhibiting angiotensin II-induced DNA synthesis in vascular smooth muscle cells.[39] The non-significant tendency for protection observed here might not necessarily be due to lowering of blood pressure because prazosin and doxazosin *per se* have been reported to exert antitumor activity against prostate cancer cells.[40,41]

Spontaneously hypertensive rats are one of the most widely accepted animal models of human essential hypertension, having been characterized as closely paralleling the human disorder in its hemodynamic, endocrine, and end-organ manifestations. Systolic blood pressure in SHR is usually between 180–200 mmHg at around 5–6 weeks of age,[42,43] and (TRAP × SHR)F1 rats in the present study showed 170–190 mmHg. Although this level of blood pressure is much higher than patients with hypertension, it is possible to apply the current data to human patients because the control (TRAP × WKY)F1 rats exhibited 140 to 160 mmHg which is also higher than that in human cases, and the blood pressure levels in the SHR is significantly higher than that of control.

The enhancement of the prostate cancer risk in SHR rats was possibly induced due to the genetic predisposition of SHR rather than hypertension *per se*. Increased RhoA expression in vascular smooth muscle cells was constantly found in SHR compared with WKY rats[44,45] and RhoA activation was significantly reduced by the treatment of valsartan, an angiotensin II receptor type I blocker (ARB), but not by prazosin.[44] Recently, we observed a significant suppressive effect of ARBs on the prostate carcinogenesis in TRAP rats (Takahashi *et al.*, unpublished data). RhoA signaling is reported to be involved in the proliferation, migration or

Table 4 Incidence and multiplicity of microinvasive adenocarcinoma

Group	Treatment	No. of rats	Ventral		Lateral		Anterior	
			Incidence	Multiplicity (/rat)	Incidence	Multiplicity (/rat)	Incidence	Multiplicity (/rat)
1	(TRAP × SHR)F1	9	4	0.56 ± 0.73	1	0.33 ± 1.00	8	1.11 ± 0.60
2	(TRAP × SHR)F1 / Prazosin	8	2	0.37 ± 0.74	2	0.25 ± 0.46	7	1.00 ± 0.53
3	(TRAP × WKY)F1	9	2	0.22 ± 0.44	1	0.11 ± 0.33	8	1.11 ± 0.60
4	(TRAP × WKY)F1 / Prazosin	8	0	–	2	0.25 ± 0.46	6	1.25 ± 0.89

TRAP, transgenic rat for adenocarcinoma of prostate; SHR, spontaneously hypertensive rat; WKY, Wistar Kyoto.

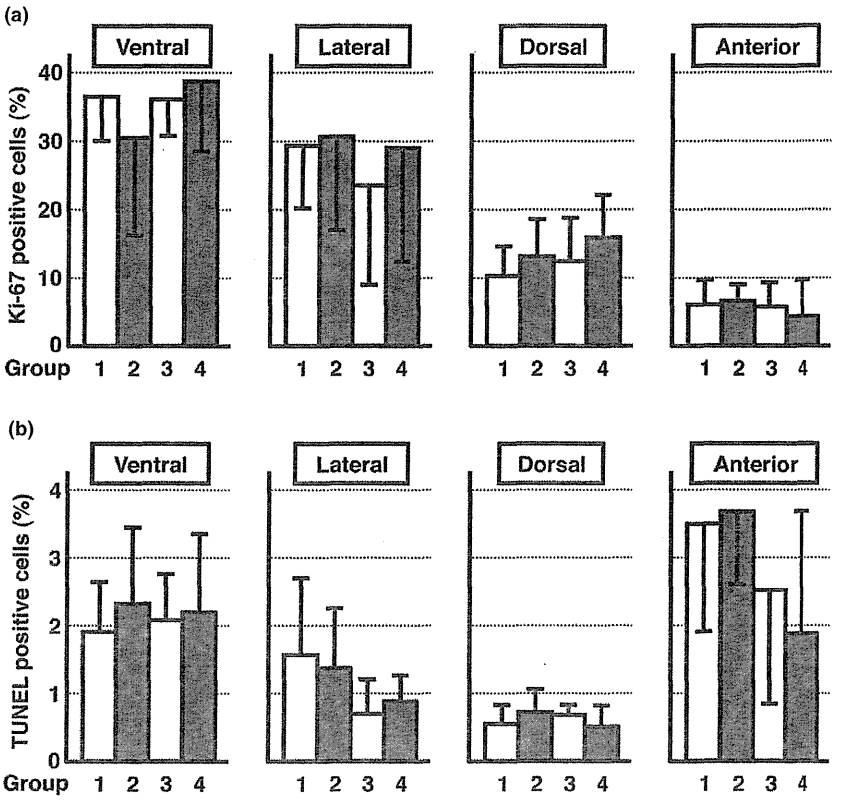

Figure 4 Labeling indices for (**a**) Ki-67 and (**b**) apoptotic cells (terminal deoxynucleotidyl transferase-mediated dUTP nick end labeling (TUNEL)) in individual prostatic lobes in Experiment 2.

metastasis of prostate cancer cells.[46,47] Therefore, it is speculated that RhoA restrictedly contributed to the progression from HG-PIN to adenocarcinoma but not from LG-PIN to HG-PIN in the present experimental condition because the RhoA signaling pathway is involved in relatively late-stage of prostate carcinogenesis.

In conclusion, the present animal experiment provided some evidence supporting the conclusion that development of hypertension contributes to increased prostate cancer risk.

ACKNOWLEDGMENTS

This work was supported by Grant-in-Aid for Cancer Research from the Ministry of Health, Labour and Welfare of Japan and a grant from the Society for Promotion of Pathology of Nagoya, Japan.

REFERENCES

1 Coleman MP, Quaresma M, Berrino F *et al.* Cancer survival in five continents: A worldwide population-based study (CONCORD). *Lancet Oncol* 2008; **9**: 730–56.
2 Franceschi S, La Vecchia C. Cancer epidemiology in the elderly. *Crit Rev Oncol Hematol* 2001; **39**: 216–26.
3 Bostwick DG, Burke HB, Djakiew D *et al.* Human prostate cancer risk factors. *Cancer* 2004; **101**: 2371–490.
4 Patel AR, Klein EA. Risk factors for prostate cancer. *Nat Clin Pract Urol* 2009; **6**: 87–95.
5 Witte JS. Prostate cancer genomics: Towards a new understanding. *Nat Rev Genet* 2009; **10**: 77–82.
6 Shirai T, Asamoto M, Takahashi S, Imaida K. Diet and prostate cancer. *Toxicology* 2002; **181–182**: 89–94.

7 Lophatananon A, Archer J, Easton D *et al.* Dietary fat and early-onset prostate cancer risk. *Br J Nutr* 2010; **103**: 1375–80.
8 Zheng W, Lee SA. Well-done meat intake, heterocyclic amine exposure, and cancer risk. *Nutr Cancer* 2009; **61**: 437–46.
9 Buell P, Dunn JE Jr. Cancer mortality among Japanese ISSEI and NISEI of California. *Cancer* 1965; **18**: 656–64.
10 Shimizu H, Ross RK, Bernstein L, Yatani R, Henderson BE, Mack TM. Cancers of the prostate and breast among Japanese and white immigrants in Los Angeles County. *Br J Cancer* 1991; **63**: 963–66.
11 Ito N, Hasegawa R, Sano M *et al.* A new colon and mammary carcinogen in cooked food, 2-amino-1-methyl-6-phenylimidazo[4,5-b]pyridine (PhIP). *Carcinogenesis* 1991; **12**: 1503–06.
12 Shirai T, Sano M, Tamano S *et al.* The prostate: A target for carcinogenicity of 2-amino-1-methyl-6-phenylimidazo[4,5-b]pyridine (PhIP) derived from cooked foods. *Cancer Res* 1997; **57**: 195–98.
13 Inaguma S, Takahashi S, Ohnishi H, Suzuki S, Cho YM, Shirai T. High susceptibility of the ACI and spontaneously hypertensive rat (SHR) strains to 2-amino-1-methyl-6-phenylimidazo[4,5-b]pyridine (PhIP) prostate carcinogenesis. *Cancer Sci* 2003; **94**: 974–79.
14 Asamoto M, Hokaiwado N, Cho YM *et al.* Prostate carcinomas developing in transgenic rats with SV40 T antigen expression under probasin promoter control are strictly androgen dependent. *Cancer Res* 2001; **61**: 4693–700.
15 Cho YM, Takahashi S, Asamoto M *et al.* Age-dependent histopathological findings in the prostate of probasin/SV40 T antigen transgenic rats. Lack of influence of carcinogen or testosterone treatment. *Cancer Sci* 2003; **94**: 153–57.
16 Seeni A, Takahashi S, Takeshita K *et al.* Suppression of prostate cancer growth by resveratrol in the transgenic rat for adenocarcinoma of prostate (TRAP) model. *Asian Pac J Cancer Prev* 2008; **9**: 7–14.
17 Golomb E, Rosenzweig N, Eilam R, Abramovici A. Spontaneous hyperplasia of the ventral lobe of the prostate in aging genetically hypertensive rats. *J Androl* 2000; **21**: 58–64.
18 Martin RM, Vatten L, Gunnell D, Romundstad P. Blood pressure and risk of prostate cancer: Cohort Norway (CONOR). *Cancer Causes Control* 2010; **21**: 463–72.
19 Beebe-Dimmer JL, Dunn RL, Sarma AV, Montie JE, Cooney KA. Features of the metabolic syndrome and prostate cancer in African-American men. *Cancer* 2007; **109**: 875–81.
20 Friedman GD. Blood pressure, and heart rate: No evidence for a positive association with prostate cancer. *Ann Epidemiol* 1997; **7**: 486–89.
21 Stocks T, Hergens MP, Englund A, Ye W, Stattin P. Blood pressure, body size and prostate cancer risk in the Swedish Construction Workers cohort. *Int J Cancer* 2010; **127**: 1660–68.
22 Harris AM, Warner BW, Wilson JM *et al.* Effect of alpha1-adrenoceptor antagonist exposure on prostate cancer incidence: An observational cohort study. *J Urol* 2007; **178**: 2176–80.
23 Lever AF, Hole DJ, Gillis CR *et al.* Do inhibitors of angiotensin-I-converting enzyme protect against risk of cancer? *Lancet* 1998; **352**: 179–84.
24 Perron L, Bairati I, Harel F, Meyer F. Antihypertensive drug use and risk of prostate cancer (Canada). *Cancer Causes Control* 2004; **15**: 535–41.
25 Friis S, Sorensen HT, Mellenkjaer L *et al.* Angiotensin-converting enzyme inhibitors and the risk of cancer. A population-based cohort study in Denmark. *Cancer* 2001; **92**: 2462–70.
26 Lindholm LH, Anderson H, Ekbom T *et al.* Relation between drug treatment and cancer in hypertensives in the Swedish Trial in Old Patients with Hypertension 2: A 5-year, prospective, randomised, controlled trial. *Lancet* 2001; **358**: 539–44.
27 Reckelhoff JF. Gender differences in the regulation of blood pressure. *Hypertension* 2001; **37**: 1199–208.
28 Ganten U, Schroder G, Witt M, Zimmermann F, Ganten D, Stock G. Sexual dimorphism of blood pressure in spontaneously hypertensive rats: Effects of anti-androgen treatment. *J Hypertens* 1989; **7**: 721–26.
29 Reckelhoff JF, Zhang H, Srivastava K, Granger JP. Gender differences in hypertension in spontaneously hypertensive rats. Role of androgens and androgen receptor. *Hypertension* 1999; **34**: 920–23.
30 Reckelhoff JF, Zhang H, Granger JP. Testosterone exacerbates hypertension and reduces pressure-natriuresis in male spontaneously hypertensive rats. *Hypertension* 1998; **31**: 435–39.
31 Reckelhoff JF, Zhang H, Srivastava K. Gender differences in development of hypertension in spontaneously hypertensive rats. Role of the renin-angiotensin system. *Hypertension* 2000; **35**: 480–83.
32 Rigat B, Hubert C, Alhenc-Gelas F, Cambien F, Corvol P, Soubrier F. An insertion/deletion polymorphism in the angiotensin I-converting enzyme gene accounting for half the variance of serum enzyme levels. *J Clin Invest* 1990; **86**: 1343–46.
33 Sayed-Tabatabaei FA, Schut AFC, Hofman A *et al.* A study of gene-environment interaction on the gene for angiotensin converting enzyme: A combined functional and population based approach. *J Med Genet* 2004; **41**: 99–103.
34 Nara Y, Nabika T, Ikeda K, Sawamura M, Endo J, Yamori Y. Blood pressure cosegregates with a microsatellite of angiotensin I converting enzyme (ACE) in F2 generation from a cross between original normotensive Wistar-Kyoto rat (WKY) and stroke-prone spontaneously hypertensive rat (SHRSP). *Biochem Biophys Res Commun* 1991; **181**: 941–46.
35 Tremblay J, Hum DHF, Sanchez R *et al.* TA repeat variation, *Npr1* expression, and blood pressure. Impact of the *Ace* locus. *Hypertension* 2003; **41**: 16–24.
36 Zhang L, Summers KM, West MJ. Angiotensin I converting enzyme gene cosegregates with blood pressure and heart weight in F2 progeny derived from spontaneously hypertensive and normotensive Wistar-Kyoto rats. *Clin Exp Hypertens* 1996; **18**: 753–71.
37 Sierra Diaz E, Sanchez Corona J, Rosales Gomez RC *et al.* Angiotensin-converting enzyme insertion/deletion and angiotensin type 1 receptor A1166C polymorphisms as genetic risk factors in benign prostatic hyperplasia and prostate cancer. *J Renin Angiotensin Aldosterone Syst* 2009; **10**: 241–46.
38 Yigit B, Bozkurt N, Narter F, Yilmaz H, Yucebas E, Isbir T. Effects of ACE I/D polymorphism on prostate cancer risk, tumor grade and metastasis. *Anticancer Res* 2007; **27**: 933–36.
39 van Kleef EM, Smits JFM, De Mey JGR *et al.* Alpha1-adrenoreceptor blockade reduces the angiotensin II-induced vascular smooth muscle cell DNA synthesis in the rat thoracic aorta and carotid artery. *Circ Res* 1992; **70**: 1122–27.
40 Garrison JB, Kyprianou N. Doxazosin induces apoptosis of benign and malignant prostate cells via a death receptor-mediated pathway. *Cancer Res* 2006; **66**: 464–72.
41 Lin SC, Chueh SC, Hsiao CJ *et al.* Prazosin displays anticancer activity against human prostate cancers: Targeting DNA and cell cycle. *Neoplasia* 2007; **9**: 830–39.
42 Trippodo NC, Frohlich ED. Similarities of genetic (spontaneous) hypertension. Man and rat. *Circ Res* 1981; **48**: 309–19.
43 Pinto YM, Paul M, Ganten D. Lessons from rat models of hypertension: From Goldblatt to genetic engineering. *Cardiovasc Res* 1998; **39**: 77–88.

44 Moriki N, Ito M, Seko T *et al.* RhoA activation in vasucular smooth muscle cells from stroke-prone spontaneously hypertensive rats. *Hypertens Res* 2004; **27**: 263–70.
45 Seasholtz TM, Zhang T, Morissette MR, Howes AL, Yang AH, Brown JH. Increased expression and activity of RhoA are associated with increased DNA synthesis and reduced $p27^{Kip1}$ expression in the vasculature of hypertensive rats. *Circ Res* 2001; **89**: 488–95.
46 Grandoch M, Rose A, ter Braak M *et al.* Epac inhibits migration and proliferation of human prostate carcinoma cells. *Br J Cancer* 2009; **101**: 2038–42.
47 Senapati S, Rachagani S, Chaudhary K, Johansson SL, Singh RK, Batra SK. Overexpression of macrophage inhibitory cytokine-1 induces metastasis of human prostate cancer cells through the FAK-Rho A signaling pathway. *Oncogene* 2010; **29**: 1293–302.

Cancer Letters 306 (2011) 142–150

Contents lists available at ScienceDirect

Cancer Letters

journal homepage: www.elsevier.com/locate/canlet

Induction of G1 arrest and apoptosis in androgen-dependent human prostate cancer by Kuguacin J, a triterpenoid from *Momordica charantia* leaf

Pornsiri Pitchakarn [a,d], Shugo Suzuki [a], Kumiko Ogawa [a,b], Wilart Pompimon [c], Satoru Takahashi [a], Makoto Asamoto [a], Pornngarm Limtrakul [d,*], Tomoyuki Shirai [a,*]

[a] *Department of Experimental Pathology and Tumor Biology, Nagoya City University, Graduate School of Medical Sciences, Nagoya, Japan*
[b] *Division of Pathology, National Institute of Health Sciences, Tokyo, Japan*
[c] *Laboratory of Natural Products, Department of Chemistry, Faculty of Science, Lampang Rajabhat University, Lampang, Thailand*
[d] *Department of Biochemistry, Faculty of Medicine, Chiang Mai University, Chiang Mai 50200, Thailand*

ARTICLE INFO

Article history:
Received 18 October 2010
Received in revised form 5 February 2011
Accepted 28 February 2011

Keywords:
Prostate cancer
Apoptosis
Cell cycle
Bitter melon
Kuguacin J

ABSTRACT

In this study, we focused on the effects of a bitter melon (*Momordica charantia*) leaf extract (BMLE) and a purified component, Kuguacin J (KuJ), on androgen-dependent LNCaP human prostate cancer cells. Both treatments exerted growth inhibition through G1 arrest and induction of apoptosis. In addition, KuJ markedly decreased the levels of cyclins (D1 and E), cyclin-dependent kinases (Cdk2 and Cdk4) and proliferating cell nuclear antigen, and caused an increase in p21 and p27 levels. Its induction of apoptosis was accompanied by an increase in cleavage of caspase-3 and poly (ADP-ribose) polymerase, attributable to augment of Bax/Bcl-2 and Bad/Bcl-xL and reduction of survivin levels. BMLE and KuJ also reduced the expression of androgen receptor (AR), prostate-specific antigen (PSA) while induced P53 protein level. Down-regulation of p53 by RNA interference indicated that BMLE and KuJ inhibited cell growth partly through p53-dependent cell cycle arrest and apoptotic pathways. Both BMLE and KuJ caused less toxicity in a normal prostate cell line, PNT1A. Our results suggest that BMLE and a purified component, KuJ, from its diethyl ether fraction could be promising candidate new antineoplastic and chemopreventive agents for androgen-dependent prostate cancer and carcinogenesis.

1. Introduction

Prostate cancer is the most common male malignant tumor in Western countries [1]. The substantial associated mortality and morbidity and its limited treatment options have led to a search for novel means for prevention. Contributing risk factors include age, ethnicity, genetic factors, and diet; in fact, diet-based agent for prevention and therapy is an attractive option based on significant findings of various epidemiologic studies, which have directly linked dietary habits to various forms of cancers, including prostate cancer [2]. Therefore, identification of bioactive compounds present in diet with potential anti-cancer efficacy has been an attractive research area in recent years [3].

Generally, deregulation of cell growth and resistance to apoptosis are major defects of cancer cells, so that approaches to induce cell cycle arrest and stimulate the apoptotic machinery could be effective. Recently, dietary phytochemicals have shown promise in this regard [4,5].

The fruit and/or leaves of *Momordica charantia*, or bitter melon, are widely consumed as a vegetable and especially as a folk medicine in Asia [6,7]. Anti-cancer activity of extracts against lymphoid leukemia, lymphoma,

* Corresponding authors. Address: Department of Experimental Pathology and Tumor Biology, Nagoya City University, Graduate School of Medical Sciences, 1 Kawasumi, Mizuho-cho, Mizuho-ku, Nagoya 467-8601, Japan, Department of Biochemistry, Faculty of Medicine, Chiangmai University, 110 Intawaroros Rd., T. Suthep, A. Maung, Chiangmai 50200, Thailand. Tel.: +81 52 853 8154; fax: +81 52 842 0817 (T. Shirai), tel.: +66 53 945325 6x218; fax: +66 53 217144/894031 (P. Limtrakul).

E-mail addresses: plimtrak@med.cmu.ac.th (P. Limtrakul), tshirai@med.nagoya-cu.ac.jp (T. Shirai).

0304-3835/$ - see front matter © 2011 Elsevier Ireland Ltd. All rights reserved.
doi:10.1016/j.canlet.2011.02.041

choriocarcinoma, melanoma, breast cancer, skin tumor, prostatic cancer, squamous carcinoma of the tongue and larynx, human bladder carcinomas and Hodgkin's disease has been reported [6,8–12], possibly linked to antioxidant [13], antiviral (human immunodeficiency virus [HIV] inhibitor) [14], antidiabetic [15] and immunomodulating properties [16]. A previous study demonstrated that Thai *M. charantia* induced phase II enzymes and repressed monooxygenase whereas a Chinese variety only affected monooxygenase [17]. We have reported that a bitter melon leaf extract (BMLE) in Thailand increased the sensitivity to a chemotherapeutic agent, vinblastine, in cervical carcinoma KB-V1 cells [18] and inhibited invasion and migration of an androgen-independent rat prostate cancer cell line (PLS10) *in vitro* while decreasing lung metastasis *in vivo* [19]. Recently, fresh bitter melon extract demonstrated growth inhibitory effects on a breast cancer cell by modulating cell cycle regulatory genes and enhancing apoptosis [20]. Our previously study, bioguided fractionation was used to identify the active component of BMLE, which is able to modulate the function of P-glycoprotein (ABCB1) and the multidrug resistance (MDR) phenotype. We found that Kuguacin J (KuJ) inhibited P-glycoprotein-mediated MDR and increased sensitivity to vinblastine and paclitaxel in KB-V1 cells [21]. In the present study, for the first time, effects of BMLE against an androgen-dependent human prostate cancer cell line, LNCaP, *in vitro* were examined. Since BMLE is crude extract, we also focused on KuJ, a purified component.

2. Materials and methods

2.1. Plant material and extraction [21]

Bitter melon leaves were collected in Lampang province, Thailand, in March 2009. A voucher specimen (BKF No. 15602) has been deposited at the Forest Herbarium, Department of National Park, Wildlife and Plant Conservation, Ministry of Natural Resources and Environment, Bangkok, Thailand. Fresh leaves were dried at 30–45 °C, ground and powdery plant samples (1 kg) were extracted exhaustively with 4 L of 80% ethanol by maceration at 37 °C for 16 h. The mixture was filtered and re-extracted with 4 L of ethanol. The combined filtrate was bleached with 160 g of active charcoal, filtered and concentrated by rotary evaporation to 120 mL before filtering to remove precipitates. The filtrate was rotary evaporated and lyophilized twice to obtain BMLE (65.37 g) then kept at −20 °C protected from light. BMLE was dissolved in a final DMSO concentration adjusted to 0.1% (v/v) in the culture medium.

For isolation of KuJ, 100 g of BMLE was re-dissolved in 1 L of 50% methanol and successively partitioned with hexane (0.58 g), diethyl ether (13.32 g), chloroform (4.63 g), ethyl acetate (3.65 g) and an aqueous layer. Each fraction was dried under reduced pressure and then submitted to bioassays. A portion of the diethyl ether fraction (15 g) was chromatographed in a silica gel 60 (Merck KGaA, Darmstadt, Germany) column, eluting in sequence with an increasing concentration of hexane in ethyl acetate. Further separation by silica gel 60 F254 preparative thin layer chromatography using hexane in ethyl acetate (90:10) as a mobile phase led to isolation of KuJ (1.23 g). The compound was identified as the previously described triterpenoid, KuJ, by comparison of its physical and HPLC, IR, MS and NMR data with those reported in the literature [21–25]. The purified KuJ ($C_{30}H_{46}O_3$, purity >99.99% by high-resolution mass spectrometry) with a molecular weight of 454 (Fig. 2B) was dissolved in DMSO as a stock solution, and used directly in the cell culture treatments. The percentage composition of KuJ included in BMLE and the organic fraction (diethyl ether) was analyzed by HPLC.

2.2. Cell culture

An androgen-dependent human prostate cancer cell line, LNCaP, was purchased from The American Type Culture Collection (ATCC, Manassas, VA, USA) and a human normal prostatic epithelial cell line, PNT1A, from the Health Protection Agency Culture Collections (Salisbury, United Kingdom). The cells was cultured in Roswell Park Memorial Institute-1640 Medium (RPMI 1640, Gibco, Carlsbad, CA, USA) with 10% fetal bovine serum (FBS, Life Technologies Japan Ltd., Japan), 50 U/ml penicillin and 50 μg/ml streptomycin, in a humidified incubator with an atmosphere comprising 95% air and 5% CO_2 at 37 °C. When the cells reached 70–80% confluence, they were harvested and plated either for subsequent passage or for treatment. DMSO was used as a vehicle control in all experiment and adjusted to the final concentration at 0.1% in culture medium. The following experiments were performed in triplicate.

2.3. Cytotoxicity and growth inhibition assays

LNCaP cells were plated at 5.0×10^3 cells per well in 96-well plates. Twenty-four hours after plating, various concentrations of BMLE or KuJ were added. The cells were then incubated for 24 and 48 h at 37 °C, and cell growth were assessed by WST-1 colorimetric assay (Roche Diagnostics, Mannheim, Germany) [26].

2.4. Cell cycle analysis

The cells were treated with BMLE or KuJ at various concentrations for 24 or 48 h then suspensions were prepared and stained with propidium iodide (Guava® cell cycle reagent, Guava Technologies) according to the Guava® Cell Cycle Assay protocol. Cell cycle phase distributions were determined on a Guava® PCA Instrument using CytoSoft Software.

2.5. Apoptosis assays

Apoptosis was assessed using the Guava® Nexin reagent and the Guava® PCA system (Guava Technologies, Hayward, CA, USA). The Guava® Nexin assay utilizes two stains (annexin V and 7-amino actinomycin D [7-AAD]) to quantitate the percentage of apoptotic cells. It was performed according to the manufacturer's protocol. After treatment with BMLE or KuJ for 24 or 48 h, cell suspensions were

prepared and stained with Guava® Nexin reagent for 20 min and immediately processed with the Guava PCA system. Cells were gated based on forward scatter (size), and results reported as the percentage of gated cells positive for both annexin V and 7-AAD.

2.6. Immunoblot analyses

After treatment, cells were washed twice with ice-cold phosphate buffer saline (PBS), scraped with a cell scraper into ice-cold PBS and centrifuged at 1500 rpm for 10 min. The supernatant was removed and cell pellets were lysed with a RIPA buffer (Pierce Biotechnology, Rockford, Illinois, USA) containing a protease inhibitor (Pierce Biotechnology) for 15 min on ice. The insoluble matter was removed by centrifugation at 12,000 rpm for 20 min at 4 °C and supernatants were collected. Protein concentrations were determined with a Coomassie Plus™-The Better Bradford Assay Kit (Pierce Biotechnology).

Samples were mixed with 2× sample buffer (Bio-Rad Laboratories, Hercules, California USA) and heated for 5 min at 95 °C and then subjected to 10% SDS–PAGE. The separated proteins were transferred onto nitrocellulose membranes followed by blocking with 5% nonfat milk powder (w/v) in 1× TBS [10 mmol/L Tris–HCl (pH7.5), 100 mmol/L NaCl, 0.1% Tween-20] for 1 h at room temperature. Membranes were probed with antibodies for AR, Bax, cyclin D1, cyclin E, p21, p27, proliferating cell nuclear antigen (PCNA) (Santa Cruz Biotechnology, Inc., Santa Cruz, CA, USA), BcL-2, prostate-specific antigen (PSA) (DAKO, Denmark A/S, Glostrup, Denmark), CDK2, CDK4 (BD Biosciences, San Jose, CA, USA), Bad, Bcl-xL, caspase-3, cleaved caspase-3, poly(ADP-ribose) polymerase (PARP), p53, and survivin (Cell Signaling, Technology Inc., Danvers, Massachusetts, USA) in 5% nonfat dry milk, 1X TBS, 0.1% Tween-20 at 4 °C overnight, followed by exposure to peroxidase-conjugated appropriate secondary antibodies and visualization with an enhanced chemiluminescence detection system (GE Healthcare Bio-sciences, Buckinghamshire, NA, UK). To confirm equal protein loading, each membrane was stripped and reprobed with anti-β-actin (Sigma–Aldrich, Co., St. Louis, MO, USA) or anti-tubulin antibodies (Santa Cruz Biotechnology). Band density of Bad, Bax, Bcl-2, Bcl-xL and tubulin were then determined with ImageJ 1.410 (National Institute of Mental Health, Maryland, USA).

2.7. RNA interference

Cells were transfected with 20 nMol/L of control siRNA or two clones of siRNA for human p53 (Invitrogen, Carlsbad, CA, USA) using Lipofectamine™ RNAiMAX reagent (Invitrogen) for 24 h. p53 siRNA2 was used for subsequent experiments with BMLE or KuJ treatments.

2.8. Statistical analysis

All data are presented as mean ± S.D. values. Statistical analyses were conducted with Prism version 5.0 using one-way ANOVA, the Dunnett test or the Tukey's test. Statistical significance was concluded with *, **, ***: $P < 0.05$, 0.01 or 0.001, respectively.

3. Results

3.1. BMLE inhibits growth of LNCaP cells

LNCaP cells were treated with the varying concentrations (0–250 μg/ml) of BMLE for 24 h and 48 h, and its effects on cell growth were assessed by WST-1 assay. Cell growth of LNCaP was significantly inhibited by BMLE at between 25 and 250 μg/ml in a concentration-dependent manner. Inhibitory concentration (IC) 50 values were approximately 100 μg/ml and 50 μg/ml for 24 h and 48 h treatment, respectively (Fig. 1A).

3.2. BMLE induces cell cycle arrest in LNCaP cells

To explore the underlying mechanism of BMLE-induced growth suppression, cell cycle analysis was performed by Guava® cell cycle assay. BMLE-treated cells appeared to dramatically accumulate in G1 phase, especially at 150 (65%, $p < 0.01$), 200 (70%, $p < 0.001$) and 250 μg/ml (65%, $p < 0.01$), compared to control (52%), with concomitant decrease in the percentage of cells in the G2/M phase (Fig 1B and C). Cell cycle arrest began to occur from 24 h of treatment (data not shown). These results thus suggest that BMLE inhibited cell proliferation by arresting cells in the G1phase.

3.3. BMLE causes apoptotic death of LNCaP cells

In addition to cell cycle arrests, morphologic observation of BMLE-treated LNCaP cells indicated floating cells which are associated with cell death (data not shown). Guava® Nexin assays showed the treatment of LNCaP with 250 μg/ml of BMLE for 48 h resulted in significant increase in both the early and late stages of apoptosis (Fig. 1D): control (6% and 5%) and 250 μg/ml (24%, $P < 0.01$ and 34%, $P < 0.05$). It was shown that BMLE at high concentration caused inhibition of LNCaP cell growth by apoptosis induction.

3.4. Effects of BMLE on expression of cell cycle- and apoptosis-related proteins

LNCaP is an AR-positive prostate cancer cell line [27] expressing wild-type p53 [28]. As shown in Fig. 1E, BMLE (200 and 250 μg/ml) reduced its expression of AR and PSA proteins as assessed by western blotting analysis. Additionally, it was found that p53 protein expression was up-regulated after treatment with 250 μg/ml of BMLE, the concentration which caused both cell cycle arrest and induction of apoptosis.

As BMLE caused G1 arrest and apoptotic induction in LNCaP, we next examined the effect of BMLE on the expression of G1 cell cycle and apoptosis-regulatory proteins. Treatment with BMLE for 48 h also resulted in a marked reduction in the expression of cyclin D1 and PCNA in a concentration-dependent manner, as well as decrease in Bcl-2, with no effect on Bax. Besides, BMLE treatment led to the decrease of pro-caspase-3 and the increase of cleaved caspase-3 in a concentration-dependent manner (Fig. 1F). The cell cycle data shown in Fig. 1B and C coupled with the reduced expression of cyclin D1 and PCNA indicate that BMLE causes G1 arrest of LNCaP cells and the apoptosis data shown in Fig. 1F coupled with the decrease in Bcl-2 and the increase in cleaved caspase-3 indicate that BLME also induces LNCaP cells to undergo apoptosis. These data confirmed BMLE caused the inhibition of LNCaP cell growth via cell cycle arrest and apoptosis induction.

3.5. Identification of an active component in BMLE

According to Section 2, partition–extraction of BMLE using organic solvents (hexane, diethyl ether, chloroform and ethyl acetate) with increasing polarity provided four organic fractions. WST-1 assays showed growth inhibitory effects on LNCaP cells with all (Fig. 2A). The diethyl ether fraction (DEF) showed the strongest inhibitory effect on LNCaP cell growth (Fig. 2Ac), which led us to further isolate purified compound using DEF as a starting material.

The active compound in DEF was identified as KuJ (Fig. 2B), which we previously show its anti-cancer effect to modulate P-glycoprotein function and reverse cancer multidrug resistance [21,23], and this compound was further tested for influence on the growth of LNCaP cells (Fig. 2C). Treatment with KuJ for 24 h slightly decreased LNCaP cell growth, whereas treatment for 48 h significantly decreased cell growth and viability of the cancer cells with an IC50 of 15 μM.

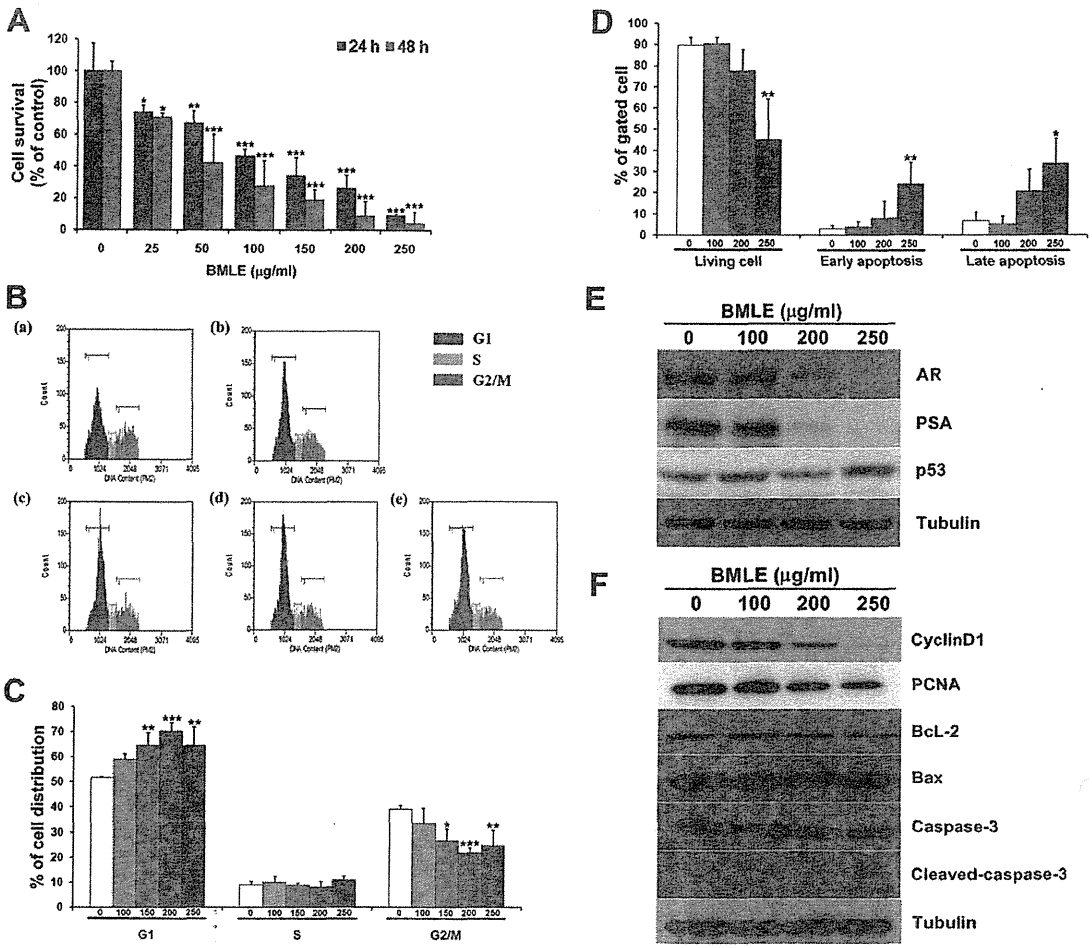

Fig. 1. BMLE caused G1 arrest and apoptosis induction in LNCaP cells. After incubation with 0–250 μg/ml BMLE for 24 and 48 h cytotoxicity was assessed by WST-1 assay (A). Histogram of cell cycle distribution (B) of LNCaP cells treated with vehicle control (a), 100 (b), 150 (c), 200 (d) and 250 (e) μg/ml BMLE for 48 h. Data analysis of cell cycle analyses (C) and apoptosis assays (D) of BMLE-treated LNCaP cells after 48 h of the treatment. The WST-1 results are expressed as percentages of vehicle control values. Data are mean ± SD values from three independent experiments. $^{*}P < 0.05$, $^{**}P < 0.01$ and $^{***}P < 0.001$, versus vehicle control. Immunoblot analysis of the protein levels of (E) AR, PSA, p53, (F) cell cycle-related proteins (cyclin D1 and PCNA) and apoptosis-related proteins (BcL-2, Bax, caspase-3 and cleaved-caspase-3) after treatment with vehicle control or BMLE for 48 h. The immunoblots shown here are representative of three independent experiments with similar results. Tubulin was employed as a loading control.

3.6. KuJ caused G1 cell cycle arrest in LNCaP cells

Based on the inhibitory effects of KuJ on LNCaP cell growth, the concentration of 15, 20, 25, and 30 μM of KuJ were selected for further *in vitro* mechanistic studies. As we found a significant effect of BMLE on cell cycle arrest in LNCaP, we thus determined the possible inhibitory effect of KuJ on cell cycle progression. As shown in Fig. 3A, treatment of LNCaP cells with KuJ for 24 and 48 h resulted in a significantly higher proportion of cells in the G1 phase at the concentrations used, 15 μM (67%, $p < 0.001$ and 64%, $p < 0.001$), 20 μM (70%, $p < 0.001$ and 69%, $p < 0.001$), 25 μM (64%, $p < 0.01$ and 63%, $p < 0.01$), and 30 μmol/L (59% and 64%, $p < 0.05$), compared with controls (55% and 53%). There was a concomitant reduction in the contributions of cells in the S and G2-M phases. These data suggest that inhibition of cell proliferation in LNCaP by KuJ might be associated with the induction of G1 arrest.

3.7. Induction of apoptosis by KuJ in LNCaP cells

To determine whether the KuJ-induced loss of the proliferation capacity and cell viability of LNCaP cells was associated with the induction of apoptosis, the cells were treated with KuJ as described above and the numbers of apoptotic cells were assessed. Apoptotic cells were counted as living cells and late or early apoptotic cells, which are presented in Fig. 3B. Treatment of KuJ for 24 h at 30 μM slightly but significantly induced apoptosis of LNCaP cells compare to controls (Fig. 3Ba). Treatment of LNCaP cells by 25 and 30 μM of KuJ for 48 h resulted in significant enhancement in the number of apoptotic cells in both the early and late stages of apoptosis (Fig. 3Bb): control (6% and 5%), 25 μM (33%, $P < 0.01$ and 15%, $P < 0.05$) and 30 μM (40%, $P < 0.01$ and 40%, $P < 0.001$).

3.8. Alteration of cell cycle- and apoptosis-related protein levels by KuJ

We next determined the expression of AR, PSA, and p53 and found that after 48 h treatment, KuJ reduced the protein expression of AR and PSA while enhancing the level of p53 in LNCaP cells in a concentration-dependent manner (Fig. 4A).

The expression of Cdk inhibitors, p21 and p27, which regulate the progression of cells in the G1 phase were assessed. Protein levels of p21 and p27 were increased following treatment with 15 and 20 μM KuJ for 48 h. On the other hand, the protein level of p21 was decreased, while the expression of p27 was still induced by treatment with 25 and 30 μM KuJ (Fig. 4B). Additionally, the expression of G1 positive regulators (cyclin D1, cyclin E, Cdk2, Cdk4 and PCNA) was down-regulated in a concentration-dependent manner (Fig. 4B).

We next determine whether the protein levels of apoptosis-involving proteins would be altered by KuJ. Treatment with KuJ at 15 and 20 μM resulted in a concentration-dependent reduction in the levels of the anti-apoptotic protein Bcl-xL with a concomitant increase in the level of pro-apoptotic protein Bad, while that of Bax was not changed (Fig. 4C). KuJ treatment at 25 and 30 μM dramatically decreased the protein

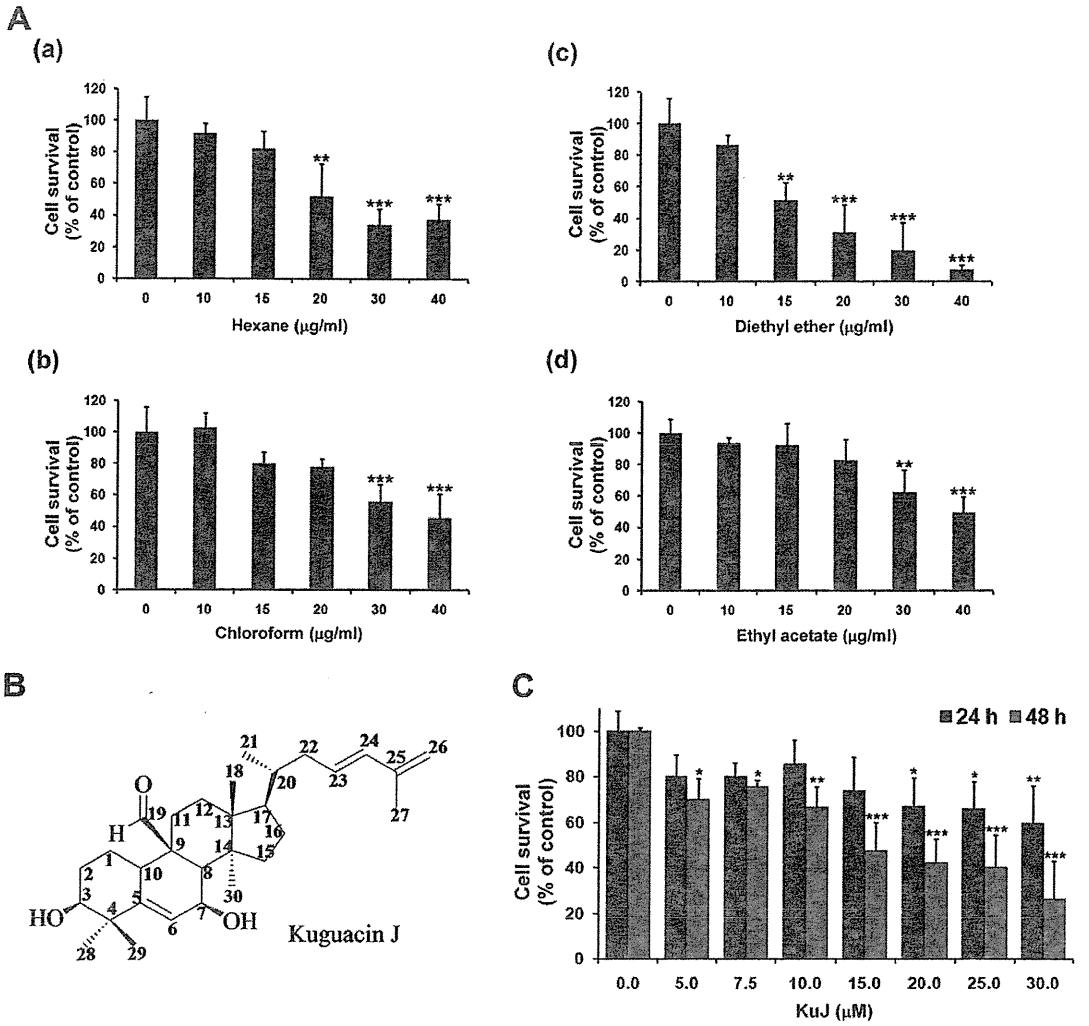

Fig. 2. Characterization of an active component in BMLE. (A) Cells were treated with 0–40 μg/ml of organic fractions obtained by partition–extraction using: (a) hexane, (b) diethyl ether, (c) chloroform and (d) ethyl acetate for 48 h and then WST-1 assays were perform to determine their growth inhibitory effects. (B) Structural formula of KuJ. (C) KuJ showed growth suppression in LNCaP cells as demonstrated by the WST-1 assay. The results are expressed as percentages of the vehicle control group value. Data are mean ± SD values from three independent experiments. $^{*}P < 0.05$, $^{**}P < 0.01$ and $^{***}P < 0.001$, versus control.

expression of Bcl-xL and Bcl-2 and slightly reduced the level of Bad and Bax. Band density analyses indicated that while KuJ treatment caused an overall decrease in expression of pro-apoptotic proteins, at the same time it elevated the ratios of Bax/Bcl-2 and Bad/Bcl-xL, which could initiate the caspase activation pathway for apoptosis (Data not shown) Likewise, KuJ treatment at dose of 25 and 30 μM, dramatically decreased the expression of survivin and caspase-3 and increased the expression of cleaved caspase-3 accompanied by cleavage of PARP.

The results demonstrated that KuJ altered the expressions of cell cycle- and apoptosis-regulatory proteins contributed to G1 arrest and apoptosis induction in LNCaP cells.

3.9. p53-dependent cell cycle arrest and apoptosis induction by KuJ in LNCaP cells

The induction of p53 might be a one possibility for BMLE and KuJ to trigger LNCaP cell growth. To investigate this mechanism, the cells were transfected with p53 siRNA follow by BMLE or KuJ treatment. The efficiency of p53 siRNA was proven with reference to decrease of p53 protein expression using western blotting analysis, and the expression of p21, a downstream target of p53 also was determined (Fig. 5A). In LNCaP cells, p53 protein expression was knocked down by treatment of p53 siRNA for 24 h compared with the control siRNA. Then the cells were treated with BMLE (250 μg/ml) or KuJ (25 μM) and the percentage cell distribution and apoptotic cell death were determined. As shown in Fig. 5B and C, transfection of p53 siRNA in LNCaP cells significantly reversed BMLE-induced cell cycle arrest, but slightly decreased KuJ-induced arrest of the cell cycle. Furthermore, the increase of the number of apoptotic cells by BMLE and KuJ was dramatically reduced when the cells were pre-treated with p53 siRNA (Fig. 5D and E).

3.10. Cytotoxicity of BMLE and KuJ in PNT1A cells

PNT1A cells were treated with various concentrations of BMLE or KuJ for 24 h and 48 h, and cell viability were assessed by WST-1 assay. With BMLE treatment, the viability of the cells was significantly reduced at concentrations between 200 and 250 μg/ml. The IC 50 values for BMLE were approximately 100 μg/ml and 50 μg/ml for 24 h and 48 h treatment, respectively (Fig. 6A). Cell viability was significantly decreased by KuJ at concentrations between 25 and 30 μM for 24 h and 20–30 μM for 48 h treatment. The IC 50 was more than 30 μM for both 24 h and 48 h treatment, (Fig. 6B). In contrast to the effect of BMLE and KuJ in cancer cell line, LNCaP, the results showed that the both compounds caused less toxicity in non-neoplastic human prostate epithelial cells.

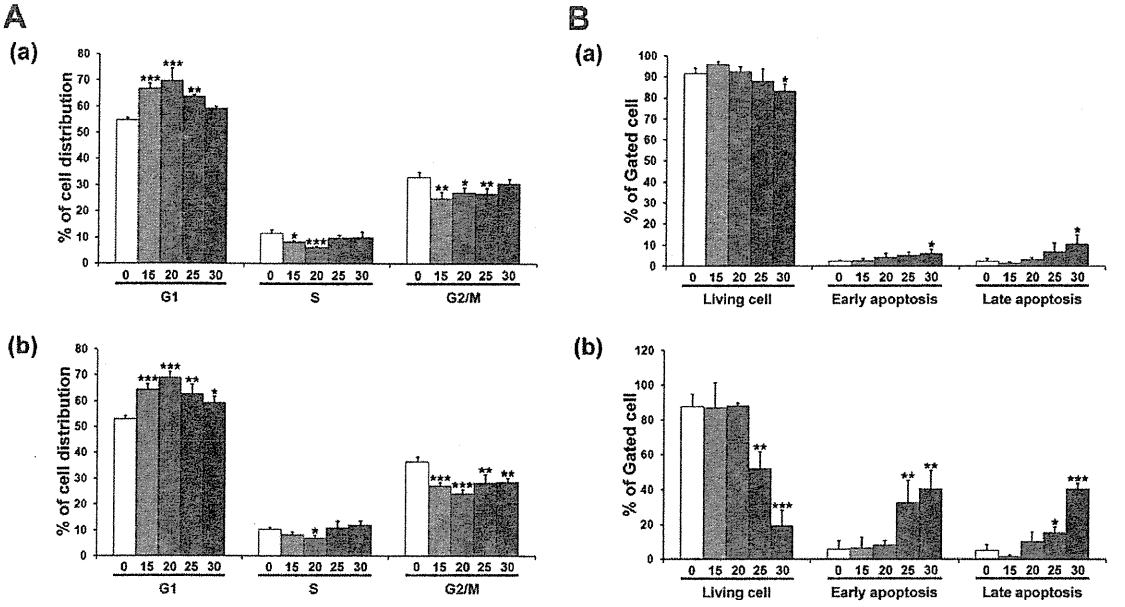

Fig. 3. Effects of KuJ on cell cycle progression and apoptosis induction in LNCaP cells. After treatment with 0, 15, 20, 25 and 30 μM KuJ, cells were harvested for analysis of cell cycle distribution and apoptosis. (A) LNCaP cell cycle distribution after treatment with KuJ for 24 (a) and 48 h (b). (B) Percentage of living cells, early and late apoptoses were summarized after 24 (a) and 48 h (b) of KuJ treatment. Data are mean ± SD values from three independent experiments. $^{*}P < 0.05$, $^{**}P < 0.01$ and $^{***}P < 0.001$, versus vehicle control.

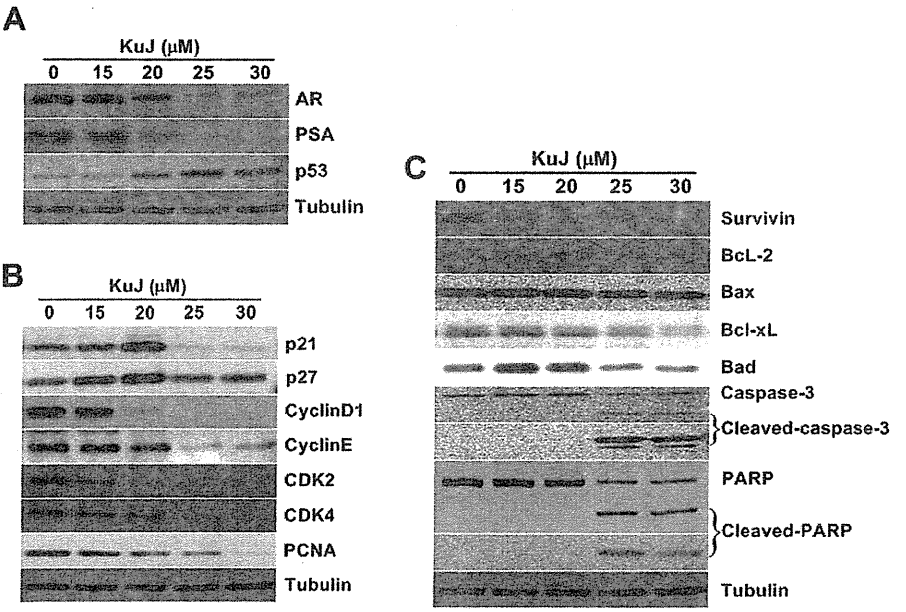

Fig. 4. KuJ alteration of the expression of cell cycle- and apoptosis-involving proteins. Immunoblot analysis of the protein levels of AR, PSA, p53 (A), cell cycle-related proteins (p21, p27, cyclin D1, cyclinE, CDK2, CDK4 and PCNA); (B) and apoptosis-related proteins (survivin, BcL-2, Bax, Bcl-xL, Bad, caspase-3, cleaved-caspase-3, PARP and cleaved-PARP); (C) after treatment with vehicle control or KuJ for 48 h. The immunoblots shown here are representative of three independent experiments with similar results. Tubulin was employed as a loading control.

4. Discussion

Fruits, vegetables, and common beverages, as well as several herbs and plants with diversified pharmacological properties, have been shown to be rich sources of micro-chemicals with the potential to prevent human cancers [29,30]. Prostate cancer is an ideal disease for chemopreventive intervention as it grows slowly before the onset of symptoms and the establishment of diagnosis, which usually occurs in men more than 50 years of age. Therefore, pharmacological or nutritional intervention could considerably impact the quality of life of patients by delaying the progression of cancer [5]. The present study found that BMLE exerted significant growth inhibitory

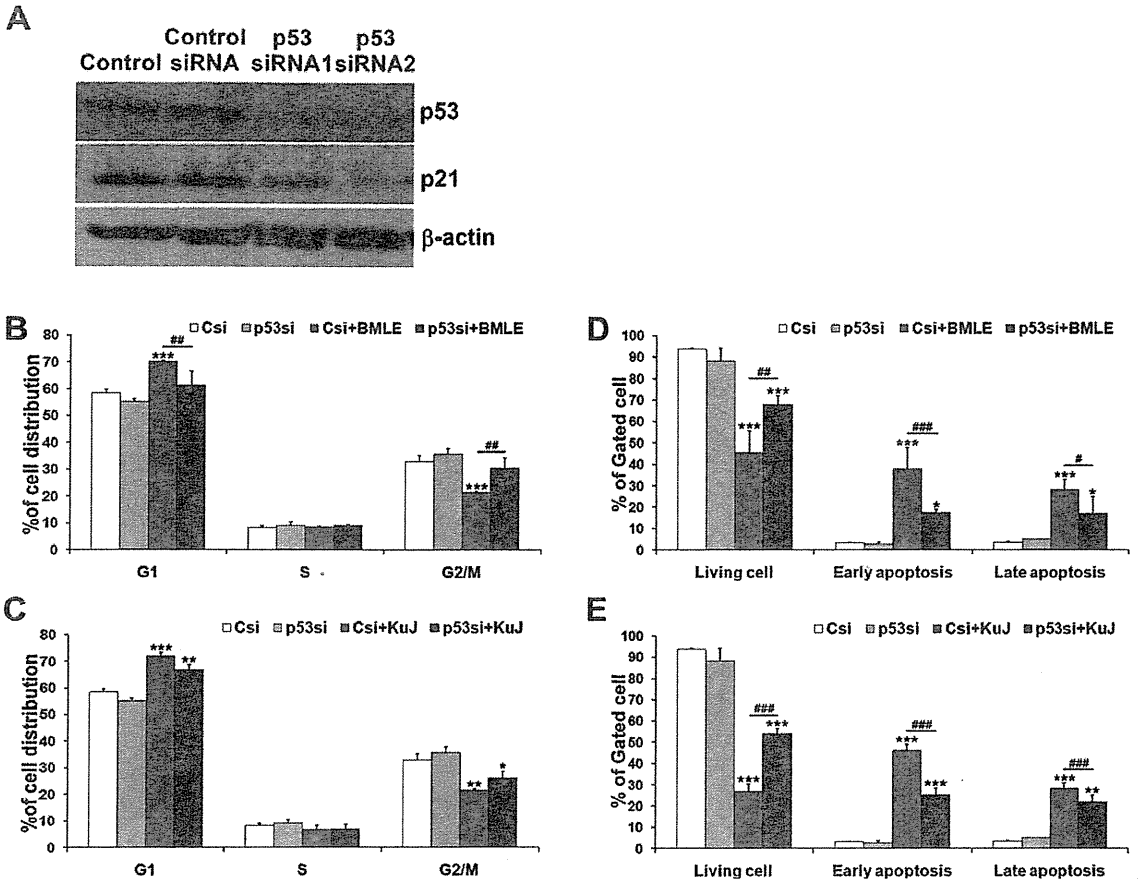

Fig. 5. BMLE and KuJ induction of p53-mediated cell cycle arrest and apoptosis in LNCaP. (A) Efficiency of p53 knockdown by 20 nM p53 siRNA was verified using Western blotting at 24 h post transfection. Cell cycle distribution and apoptosis were estimated when siRNA-transfected LNCaP cells were treated with (B and D) 250 μg/ml BMLE and (C and E) 25 μM KuJ. Data are mean ± SD values from three independent experiments. * or $^{\#}P < 0.05$, ** or $^{\#\#}P < 0.01$ and *** or $^{\#\#\#}P < 0.001$, versus control.

effects on LNCaP cells via induction of G1 arrest and apoptosis cell death. Thus identification of anti-cancer component(s) in BMLE could be valuable for prevention and intervention of cancers and the partition–extraction yielded four organic fractions, among which, DEF exerted the highest growth inhibitory effects. After the isolation using DEF as a starting material, KuJ, a known triterpenoid was obtained which also caused dramatic decrease of LNCaP cell proliferation and viability, indicating that it is at least one active component in BMLE.

Regulation of cell cycle progression in cancer cells is considered to be a potentially effective mechanism for control of tumor growth [31,32]. Molecular analyses of human cancers have revealed that cell cycle regulators frequently often display abnormalities in encoding genes in most common malignancies [33,34]. Here, treatment of androgen-sensitive (LNCaP) cells with KuJ resulted in significant G1-phase arrest of cell cycle progression, along with reduction of cyclin D1, cyclinE, Cdk2 and Cdk4 and increase of p21 and p27 at the protein level. This indicates the KuJ-induced G1 arrest might be mediated through the up-regulation of p21 and p27 proteins, which enhance the formation of heterotrimeric complexes with G1-S Cdks and cyclins, thereby inhibiting their activity. Additionally, KuJ also dramatically suppressed the expression of a proliferation marker, PCNA, that is expressed in late G1 phase and early S phase [35]. The inhibition of cell proliferation or the induction of cell death in LNCaP by KuJ might be associated with G1 arrest machinery.

G1-phase arrest of cell cycle progression provides an opportunity for cells to either undergo repair or follow the apoptotic pathway, which plays a crucial role in tissue homeostatic eliminating mutated hyperproliferating neoplastic cells from the system. Acquired resistance toward apoptosis is a hallmark of most and perhaps all types of cancer. Therefore induction of apoptosis is considered to be one of protective mechanisms against cancer progression. In the present study, treatment of LNCaP cells with 25 and 30 μM of KuJ resulted in significant induction of apoptosis. Survivin is a member of the inhibitor of apoptosis protein family, involved in inhibition of apoptosis, exerts multiple effects throughout the cell cycle [36]. Our study revealed that KuJ treatment reduced the protein level of survivin, which might be associated with KuJ-induced cell cycle arrest and apoptosis in LNCaP cells. In addition, since the ratios of pro-apoptotic proteins (e.g., Bad and Bax) and anti-apoptotic proteins (e.g., Bcl-2 and Bcl-xL) are essential for the regulation of apoptosis through

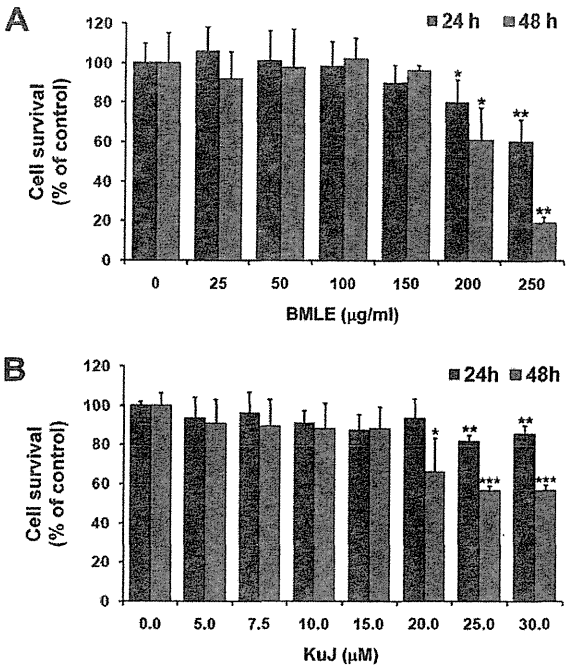

Fig. 6. Cytotoxicity of BMLE and KuJ in PNT1A cells. Cells were incubated with (A) 0–250 μg/ml BMLE or (B) 0–30 μM KuJ for 24 and 48 h and then cytotoxicity was assessed by WST-1 assay. The WST-1 results are percentages of vehicle control values. Data are mean ± SD values from three independent experiments. $^{*}P < 0.05$, $^{**}P < 0.01$ and $^{***}P < 0.001$, versus control.

caspase signaling [37], the finding that KuJ could alter the protein levels of key members of the Bcl-2 family in a manner that favors an increase in the ratios of Bax/Bcl-2 and Bad/Bcl-xLis of obvious significance.

AR is known to play a critical role in the development and progression of prostate cancer through alteration of the normal androgen axis by dysregulation of AR activity [38]. An ability of AR to cross-talk with several growth factor signaling cascades active regulation of cell cycle, apoptosis, and differentiation outcomes in prostate cancer cells has been reported [39]. The fact that KuJ decreased the expression of AR followed by reduction of protein level of PSA might be involved in KuJ-caused growth inhibition of LNCaP through the induction of G1 arrest and apoptosis.

The tumor suppressor p53 protein is a regulator of genotoxic stress that plays an important role in DNA damage response, DNA repair, cell cycle regulation, and in triggering apoptosis after cell injury [40]. Induction of apoptosis is considered to be a central to the tumor-suppressive function of p53 [41]. Knockdown of p53 by RNA interference in LNCaP slightly suppressed cell cycle arrest whereas it markedly abolished apoptosis induction by KuJ. These results indicate that KuJ induced p53-mediated partly cell cycle arrest and mainly apoptosis, which led to the inhibition of cell growth, and may be related with the activation of p53 signaling pathways.

Because KuJ was purified from BMLE, the two were compared. The growth inhibition effects of KuJ on LNCaP cells proved similar to those of BMLE. However, KuJ accounts for only approximately 1.6% of BMLE, and the effective concentration of KuJ was only 10-fold lower. Therefore, BMLE may include other compounds which also exert anti-tumor effects. Cucurbitacin B (cucB), a triterpenoid from Cucurbitaceae vegetables also found in bitter melon seeds, caused cell cycle arrest and apoptosis induction in human colon adenocarcinoma cancer cells [42]. Additionally, Rutin, a flavonoid present in bitter melon leaves, has been reported to show growth inhibition of leukemia and ovarian carcinoma cells, with anti-invasive effects on melanoma cells [43–46]. Therefore characterization of other active components present in BMLE has to be further explored.

Interestingly, the sensitivity of the human normal prostatic epithelial cell line, PNT1A, to the cytotoxic effects of BMLE and KuJ was much lower than that of LNCaP cells, pointing to potential use as effective chemopreventive agents against androgen-sensitive prostate cancer cells. In Asia people consume fruit and/or leaves of bitter melon as food [6,7] and this and other components of the diet may be linked to low incidences of prostate cancer in general [47].We have reported BMLE to inhibit the progression of androgen-independent rat prostate cancers *in vitro* and *in vivo* [19]. To provide a basis for use of KuJ as a broader antineoplastic agent for prostate cancer, further study is needed to investigate anti-cancer effects of KuJ on human androgen-independent prostate cancer.

In conclusion, we here report for the first time the ability of BMLE and KuJ to inhibit cell proliferation and viability through induction of G1-phase arrest and apoptosis on an androgen-dependent human prostate cancer cell line, while exhibiting only low toxicity in normal human prostate epithelial cells. In addition, we provide mechanistic evidence that KuJ-induced G1 arrest and apoptosis in prostate carcinoma cells might be partly mediated through enhanced expression of p53. Taking the results together, KuJ might be a promising candidate new chemopreventive agent for androgen-dependent prostate cancer.

Conflicts of interest

None declared.

Acknowledgment

This work was supported by grants from the Royal Golden Jubilee Ph.D. Program of Thailand, National Research Council of Thailand and the Society for Promotion of Pathology of Nagoya, Japan.

References

[1] H. Gronberg, Prostate cancer epidemiology, Lancet 361 (2003) 859–864.
[2] E. Bidoli, R. Talamini, C. Bosetti, E. Negri, D. Maruzzi, M. Montella, S. Franceschi, C. La Vecchia, Macronutrients, fatty acids, cholesterol and prostate cancer risk, Ann. Oncol. 16 (2005) 152–157.
[3] G.J. Kelloff, J.A. Crowell, V.E. Steele, R.A. Lubet, C.W. Boone, W.A. Malone, E.T. Hawk, R. Lieberman, J.A. Lawrence, L. Kopelovich, I. Ali, J.L. Viner, C.C. Sigman, Progress in cancer chemoprevention, Ann. N. Y. Acad. Sci. 889 (1999) 1–13.
[4] Y.J. Surh, Cancer chemoprevention with dietary phytochemicals, Nat. Rev. Cancer 3 (2003) 768–780.

[5] D.N. Syed, N. Khan, F. Afaq, H. Mukhtar, Chemoprevention of prostate cancer through dietary agents: progress and promise, Cancer Epidemiol. Biomarkers Prev. 16 (2007) 2193–2203.
[6] E. Basch, S. Gabardi, C. Ulbricht, Bitter melon (*Momordica charantia*): a review of efficacy and safety, Am. J. Health Syst. Pharm. 60 (2003) 356–359.
[7] A. Gurib-Fakim, A.H. Subratty, F. Mahomoodally, Bitter melon: an exotic vegetable with medicinal values, Nutr. Food Sci. 35 (2005) 143–147.
[8] F. Licastro, C. Franceschi, L. Barbieri, F. Stirpe, Toxicity of *Momordica charantia* lectin and inhibitor for human normal and leukaemic lymphocytes, Virchows Arch. B Cell Pathol. Incl. Mol. Pathol. 33 (1980) 257–265.
[9] T.B. Ng, W.K. Liu, S.F. Sze, H.W. Yeung, Action of alpha-momorcharin, a ribosome inactivating protein, on cultured tumor cell lines, Gen. Pharmacol. 25 (1994) 75–77.
[10] M.G. Battelli, L. Polito, A. Bolognesi, L. Lafleur, Y. Fradet, F. Stirpe, Toxicity of ribosome-inactivating proteins-containing immunotoxins to a human bladder carcinoma cell line, Int. J. Cancer 65 (1996) 485–490.
[11] C. Ganguly, S. De, S. Das, Prevention of carcinogen-induced mouse skin papilloma by whole fruit aqueous extract of *Momordica charantia*, Eur. J. Cancer Prev. 9 (2000) 283–288.
[12] Y. Sun, P.L. Huang, J.J. Li, Y.Q. Huang, L. Zhang, S. Lee-Huang, Anti-HIV agent MAP30 modulates the expression profile of viral and cellular genes for proliferation and apoptosis in AIDS-related lymphoma cells infected with Kaposi's sarcoma-associated virus, Biochem. Biophys. Res. Commun. 287 (2001) 983–994.
[13] H. Shi, M. Hiramatsu, M. Komatsu, T. Kayama, Antioxidant property of Fructus Momordicae extract, Biochem. Mol. Biol. Int. 40 (1996) 1111–1121.
[14] S. Lee-Huang, P.L. Huang, H.C. Chen, A. Bourinbaiar, H.I. Huang, H.F. Kung, Anti-HIV and anti-tumor activities of recombinant MAP30 from bitter melon, Gene 161 (1995) 151–156.
[15] M.J. Tan, J.M. Ye, N. Turner, C. Hohnen-Behrens, C.Q. Ke, C.P. Tang, T. Chen, H.C. Weiss, E.R. Gesing, A. Rowland, D.E. James, Y. Ye, Antidiabetic activities of triterpenoids isolated from bitter melon associated with activation of the AMPK pathway, Chem. Biol. 15 (2008) 263–273.
[16] J.E. Cunnick, K. Sakamoto, S.K. Chapes, G.W. Fortner, D.J. Takemoto, Induction of tumor cytotoxic immune cells using a protein from the bitter melon (*Momordica charantia*), Cell. Immunol. 126 (1990) 278–289.
[17] W.R. Kusamran, A. Ratanavila, A. Tepsuwan, Effects of neem flowers, Thai and Chinese bitter gourd fruits and sweet basil leaves on hepatic monooxygenases and glutathione S-transferase activities, and in vitro metabolic activation of chemical carcinogens in rats, Food Chem. Toxicol. 36 (1998) 475–484.
[18] P. Limtrakul, O. Khantamat, K. Pintha, Inhibition of P-glycoprotein activity and reversal of cancer multidrug resistance by *Momordica charantia* extract, Cancer Chemother. Pharmacol. 54 (2004) 525–530.
[19] P. Pitchakarn, K. Ogawa, S. Suzuki, S. Takahashi, M. Asamoto, T. Chewonarin, P. Limtrakul, T. Shirai, *Momordica charantia* leaf extract suppresses rat prostate cancer progression in vitro and in vivo, Cancer Sci. 101 (2010) 2234–2240.
[20] R.B. Ray, A. Raychoudhuri, R. Steele, P. Nerurkar, Bitter melon (*Momordica charantia*) extract inhibits breast cancer cell proliferation by modulating cell cycle regulatory genes and promotes apoptosis, Cancer Res. 70 (2010) 1925–1931.
[21] P. Pitchakarn, S. Ohnuma, K. Pintha, W. Pompimon, S. Ambudkar, P. Limtrakul, Kuguacin J isolated from *Momordica charantia* leaves inhibits P-glycoprotein (ABCB1)-mediated multidrug resistance, J. Nutr. Biochem., in press, doi:10.1016/j.jnutbio.2010.11.005.
[22] J. Chen, R. Tian, M. Qiu, L. Lu, Y. Zheng, Z. Zhang, Trinorcucurbitane and cucurbitane triterpenoids from the roots of *Momordica charantia*, Phytochemistry 69 (2008) 1043–1048.
[23] J.C. Chen, W.Q. Liu, L. Lu, M.H. Qiu, Y.T. Zheng, L.M. Yang, X.M. Zhang, L. Zhou, Z.R. Li, Kuguacins F-S, cucurbitane triterpenoids from *Momordica charantia*, Phytochemistry 70 (2009) 133–140.
[24] D.B. Mekuria, T. Kashiwagi, S. Tebayashi, C.S. Kim, Cucurbitane triterpenoid oviposition deterrent from *Momordica charantia* to the leafminer, *Liriomyza trifolii*, Biosci. Biotechnol. Biochem. 69 (2005) 1706–1710.
[25] N. Puspawati, Isolation and identification momordicin I from leaves extract of *Momordica charantia* L., J. KIMIA 2 (2008) 53–56.
[26] K. Hamasaki, K. Kogure, K. Ohwada, A biological method for the quantitative measurement of tetrodotoxin (TTX): tissue culture bioassay in combination with a water-soluble tetrazolium salt, Toxicon 34 (1996) 490–495.
[27] J.S. Horoszewicz, S.S. Leong, E. Kawinski, J.P. Karr, H. Rosenthal, T.M. Chu, E.A. Mirand, G.P. Murphy, LNCaP model of human prostatic carcinoma, Cancer Res. 43 (1983) 1809–1818.
[28] M. Burchardt, T. Burchardt, A. Shabsigh, M. Ghafar, M.W. Chen, A. Anastasiadis, A. de la Taille, A. Kiss, R. Buttyan, Reduction of wild type p53 function confers a hormone resistant phenotype on LNCaP prostate cancer cells, Prostate 48 (2001) 225–230.
[29] R.L. Thangapazham, A. Sharma, R.K. Maheshwari, Multiple molecular targets in cancer chemoprevention by curcumin, AAPS J. 8 (2006) E443–E449.
[30] N. Khan, V.M. Adhami, H. Mukhtar, Apoptosis by dietary agents for prevention and treatment of prostate cancer, Endocr. Relat. Cancer 17 (2010) R39–52.
[31] N.P. Pavletich, Mechanisms of cyclin-dependent kinase regulation: structures of Cdks, their cyclin activators, and Cip and INK4 inhibitors, J. Mol. Biol. 287 (1999) 821–828.
[32] R. Agarwal, Cell signaling and regulators of cell cycle as molecular targets for prostate cancer prevention by dietary agents, Biochem. Pharmacol. 60 (2000) 1051–1059.
[33] M. Nakanishi, M. Shimada, H. Niida, Genetic instability in cancer cells by impaired cell cycle checkpoints, Cancer Sci. 97 (2006) 984–989.
[34] W.K. Kaufmann, K.R. Nevis, P. Qu, J.G. Ibrahim, T. Zhou, Y. Zhou, D.A. Simpson, J. Helms-Deaton, M. Cordeiro-Stone, D.T. Moore, N.E. Thomas, H. Hao, Z. Liu, J.M. Shields, G.A. Scott, N.E. Sharpless, Defective cell cycle checkpoint functions in melanoma are associated with altered patterns of gene expression, J. Invest. Dermatol. 128 (2008) 175–187.
[35] G.L. Moldovan, B. Pfander, S. Jentsch, PCNA, the maestro of the replication fork, Cell 129 (2007) 665–679.
[36] D.C. Altieri, Survivin, versatile modulation of cell division and apoptosis in cancer, Oncogene 22 (2003) 8581–8589.
[37] V. Kirkin, S. Joos, M. Zornig, The role of Bcl-2 family members in tumorigenesis, Biochim. Biophys. Acta 1644 (2004) 229–249.
[38] C.A. Heinlein, C. Chang, Androgen receptor in prostate cancer, Endocr. Rev. 25 (2004) 276–308.
[39] M.L. Zhu, N. Kyprianou, Androgen receptor and growth factor signaling cross-talk in prostate cancer cells, Endocr. Relat. Cancer 15 (2008) 841–849.
[40] L.M. Rozan, W.S. El-Deiry, p53 downstream target genes and tumor suppression: a classical view in evolution, Cell Death Differ. 14 (2007) 3–9.
[41] K. Polyak, Y. Xia, J.L. Zweier, K.W. Kinzler, B. Vogelstein, A model for p53-induced apoptosis, Nature 389 (1997) 300–305.
[42] S. Yasuda, S. Yogosawa, Y. Izutani, Y. Nakamura, H. Watanabe, T. Sakai, Cucurbitacin B induces G(2) arrest and apoptosis via a reactive oxygen species-dependent mechanism in human colon adenocarcinoma SW480 cells, Mol. Nutr. Food Res. (2009).
[43] J.P. Lin, J.S. Yang, C.C. Lu, J.H. Chiang, C.L. Wu, J.J. Lin, H.L. Lin, M.D. Yang, K.C. Liu, T.H. Chiu, J.G. Chung, Rutin inhibits the proliferation of murine leukemia WEHI-3 cells in vivo and promotes immune response in vivo, Leuk. Res. 33 (2009) 823–828.
[44] H. Luo, B.H. Jiang, S.M. King, Y.C. Chen, Inhibition of cell growth and VEGF expression in ovarian cancer cells by flavonoids, Nutr. Cancer 60 (2008) 800–809.
[45] C. Martinez Conesa, V. Vicente Ortega, M.J. Yanez Gascon, M. Alcaraz Banos, M. Canteras Jordana, O. Benavente-Garcia, J. Castillo, Treatment of metastatic melanoma B16F10 by the flavonoids tangeretin, rutin, and diosmin, J. Agric. Food Chem. 53 (2005) 6791–6797.
[46] M. Zhang, N.S. Hettiarachchy, R. Horax, P. Chen, K.F. Over, Effect of maturity stages and drying methods on the retention of selected nutrients and phytochemicals in bitter melon (*Momordica charantia*) leaf, J. Food Sci. 74 (2009) C441–448.
[47] C.S. Muir, J. Nectoux, J. Staszewski, The epidemiology of prostatic cancer. Geographical distribution and time-trends, Acta Oncol. 30 (1991) 133–140.

Food and Chemical Toxicology 50 (2012) 840–847

Contents lists available at SciVerse ScienceDirect

Food and Chemical Toxicology

journal homepage: www.elsevier.com/locate/foodchemtox

Kuguacin J, a triterpeniod from *Momordica charantia* leaf, modulates the progression of androgen-independent human prostate cancer cell line, PC3

Pornsiri Pitchakarn [a,d], Shugo Suzuki [a,*], Kumiko Ogawa [a,b], Wilart Pompimon [c], Satoru Takahashi [a], Makoto Asamoto [a], Pornngarm Limtrakul [d,*], Tomoyuki Shirai [a]

[a] Department of Experimental Pathology and Tumor Biology, Nagoya City University, Graduate School of Medical Sciences, Nagoya, Japan
[b] Division of Pathology, National Institute of Health Sciences, Tokyo, Japan
[c] Laboratory of Natural Products, Department of Chemistry, Faculty of Science, Lampang Rajabhat University, Lampang, Thailand
[d] Department of Biochemistry, Faculty of Medicine, Chiang Mai University, Chiang Mai, Thailand

ARTICLE INFO

Article history:
Received 26 July 2011
Accepted 7 January 2012
Available online 15 January 2012

Keywords:
Prostate cancer
Cell growth
Invasion
Bitter melon
Kuguacin J

ABSTRACT

In this study, we focused on the *in vitro* effects of Kuguacin J (KuJ), a purified component of bitter melon (*Momordica charantia*) leaf extract (BMLE), on the androgen-independent human prostate cancer cell line PC3 and the *in vivo* effect of dietary BMLE on prostate carcinogenesis using a PC3-xenograph model. KuJ exerted a strong growth-inhibitory effect on PC3 cells. Growth inhibition was mainly through G1-arrest: KuJ markedly decreased the levels of cyclins (D1 and E), cyclin-dependent kinases (Cdk2 and Cdk4) and proliferating cell nuclear antigen. Interestingly, KuJ also dramatically decreased the levels of survivin expressed by PC3 cells. In addition, KuJ exerted anti-invasive effects on PC3 cells, significantly inhibiting migration and invasion: KuJ inhibited secretion of the active forms of MMP-2, MMP-9 and uPA by PC3 cells. In addition, KuJ treatment significantly decreased the expression of membrane type 1-MMP (MT1-MMP) by PC3 cells. *In vivo*, 1% and 5% BMLE in the diet resulted in 63% and 57% inhibition of PC3 xenograft growth without adverse effect on host body weight. Our results suggest that KuJ is a promising new candidate chemopreventive and chemotherapeutic agent for prostate cancer.

1. Introduction

Prostate cancer is the most common male malignant tumor in Western countries (Gronberg, 2003). Androgen ablation therapy is a widely used treatment during the initial stage of this disease and may produce a favorable outcome, but most patients eventually develop ablation-resistant prostate cancers with metastatic foci. Currently, there is no therapy that is able to cure progressive hormone-refractory metastatic prostate cancer. Contributing risk factors include age, ethnicity, genetic factors, and diet: epidemiologic studies have directly linked dietary habits to various forms of cancers, including prostate cancer (Bidoli et al., 2005). This makes diet-based agents for prevention and therapy as an attractive option for the control of prostate cancer.

Carcinogenesis is generally a complex and multi-step process in which distinct molecular and cellular alterations occur. A cancer chemopreventive agent could be effective at any of these classically defined stages of carcinogenesis: initiation, promotion, progression (Kaur et al., 2009; Ramos, 2008).

Multiple organ failure caused by cancer progression is the major cause of death in cancer patients. Cancer progression is a multistep process which involves a series of processes including deregulation of cell growth and resistance to apoptosis, cellular adhesion and invasion through the basement membrane, transfer via the circulation, extravasation, and proliferation at distant sites (Fidler and Kripke, 1977; Nagase and Woessner, 1999). Therefore, prevention of tumor progression is one of the primary goals of cancer prevention and control. However, agents which are currently being used for cancer therapy are generally cytotoxic, with serious side effects that can diminish the quality of life of cancer patients (Braun-Falco et al., 2006). Recently, many efforts have been made to find non- or low-cytotoxic bioactive compounds present in the diet which have potential anticancer effects (Kelloff et al., 1999). One focus is on compounds found in medicinal plants which are able to inhibit one or more steps of cancer cell progression (Lin et al., 2009; Yodkeeree et al., 2008). For example, dietary polyphenols, which are occurred naturally in many vegetables and fruits, have been reported to have chemopreventive effect by targeting the tumor

* Corresponding authors. Addresses: Department of Experimental Pathology and Tumor Biology, Nagoya City University, Graduate School of Medical Sciences, 1 Kawasumi, Mizuho-cho, Mizuho-ku, Nagoya 467-8601, Japan. Tel.: +81 52 853 8154; fax: +81 52 842 0817 (S. Suzuki); Department of Biochemistry, Faculty of Medicine, Chiang Mai University, 110 Intawaroros Rd., T. Suthep, A. Maung, Chiang Mai 50200, Thailand. Tel.: +81 6653 945325x218, +81 6653 945326x218; fax: +81 6653 217144/894031 (P. Limtrakul).

E-mail addresses: shugo@med.nagoya-cu.ac.jp (S. Suzuki), plimtrak@med.cmu.ac.th (P. Limtrakul).

0278-6915/$ - see front matter © 2012 Elsevier Ltd. All rights reserved.
doi:10.1016/j.fct.2012.01.009

necrosis factor-related apoptosis inducing ligand (TRAIL)-mediated apoptotic pathway in cancer cells (Szliszka and Krol, 2011).

Momordica charantia or bitter melon has long been used in various Asian traditional medicine systems and is commonly consumed as a vegetable (Giron et al., 1991; Lans and Brown, 1998). Anti-cancer activities of extracts of bitter melon against lymphoid leukemia, lymphoma, choriocarcinoma, melanoma, breast cancer, skin tumors, prostatic cancer, squamous carcinoma of the tongue and larynx, human bladder carcinomas and Hodgkin's disease have been reported (Basch et al., 2003; Battelli et al., 1996; Ganguly et al., 2000; Licastro et al., 1980; Ng et al., 1994; Sun et al., 2001). The anti-cancer activities are possibly linked to antioxidant (Shi et al., 1996), antiviral (human immunodeficiency virus [HIV] inhibitor) (Lee-Huang et al., 1995), antidiabetic (Tan et al., 2008) and immunomodulating properties of the extracts (Cunnick et al., 1990). We previously reported that bitter melon leaf extract (BMLE) increased the sensitivity of cervical carcinoma KB-V1 cells to the chemotherapeutic agent vinblastine (Limtrakul et al., 2004), inhibited invasion and migration of an androgen-independent rat prostate cancer cell line (PLS10) *in vitro* while decreasing lung metastasis *in vivo* (Pitchakarn et al., 2010) and suppressed the growth of an androgen-dependent human prostate cancer cell line (LNCaP) *in vitro* (Pitchakarn et al., 2011b). Using bioguided fractionation we identified the active component of BMLE as Kuguacin J (KuJ) (Pitchakarn et al., 2011a,b). We found that KuJ inhibited *P*-glycoprotein-mediated multidrug resistance (MDR) and increased sensitivity of KB-V1 cells to vinblastine (Pitchakarn et al., 2011a) and caused G1 arrest and induced apoptosis in LNCaP cells (Pitchakarn et al., 2011b). To provide a basis for the use of KuJ as a broader antineoplastic agent for cancer progression, we investigated the anti-cancer effects of KuJ on the human androgen-independent prostate cancer cell line PC3.

2. Materials and methods

2.1. Plant material and extraction

Bitter melon leaves were collected in Lampang province, Thailand, in March 2009. A voucher specimen (BKF No. 15602) has been deposited at the Forest Herbarium, Department of National Park, Wildlife and Plant Conservation, Ministry of Natural Resources and Environment, Bangkok, Thailand. Fresh leaves were dried at 30–45 °C and ground into a powder. Powdered plant samples (1 kg) were extracted exhaustively with 4 L of 80% ethanol by maceration at 37 °C for 16 h. The mixture was filtered and re-extracted with 4 L of ethanol. The combined filtrate was bleached with 160 g of active charcoal, filtered and concentrated by rotary evaporation to 120 mL. The extract was then filtered to remove precipitates. The filtrate was rotary evaporated and lyophilized twice to obtain BMLE (65.37 g) and stored at −20 °C protected from light.

KuJ was purified from BMLE as previously described (Pitchakarn et al., 2011a). Purified KuJ ($C_{30}H_{46}O_3$, purity >99.99% by high-resolution mass spectrometry: molecular weight 454 [Fig. 1A]) was dissolved in DMSO and used directly in the cell culture treatments. DMSO was used as a vehicle control in all experiment and adjusted to a final concentration of 0.1% in culture medium.

2.2. Cell culture

The PC3 cell line was purchased from The American type Culture Collection (ATCC, Manassas, VA, USA). The cells were cultured in Roswell Park Memorial Institute-1640 Medium (RPMI 1640, Gibco, Carlsbad, CA, USA) with 10% fetal bovine serum (FBS, Life Technologies Japan Ltd., Japan), 50 U/mL penicillin and 50 μg/mL streptomycin, in a humidified incubator with an atmosphere comprising 95% air and 5% CO_2 at 37 °C. When the cells reached 70–80% confluence, they were harvested and plated either for subsequent passage or for treatment.

2.3. Animals

All animal experiments were performed under protocols approved by the Institutional Animal Care and Use Committee of Nagoya City University Graduate School of Medical Sciences. Six-week-old male athymic nude mice (KSN strain) were purchased from Nihon SLC (Hamamatsu, Japan) and housed in plastic cages with hardwood chip bedding in an air-conditioned room at 23 ± 2 °C and 55 ± 5% humidity with a 12 h light/dark cycle. Oriental MF powder diet (Oriental MF, Oriental Yeast Co., Tokyo, Japan) and distilled water were available *ad libitum*.

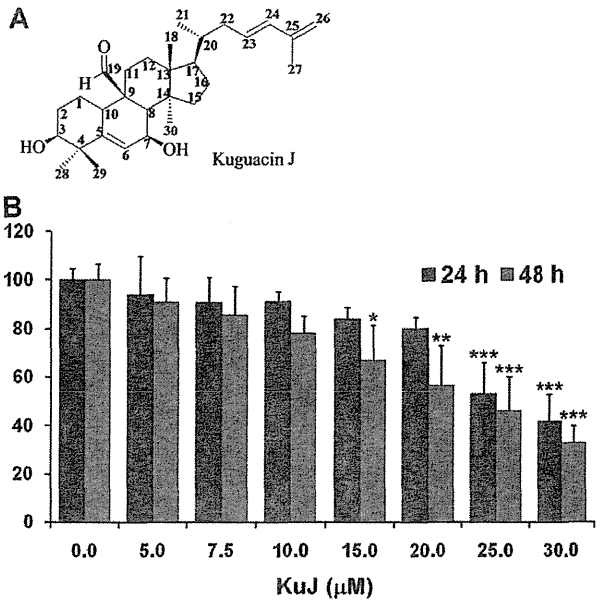

Fig. 1. Effects of KuJ on PC3 cell growth. The cells were incubated with KuJ (A) for 24 and 48 h. Cell number/viability assessed by WST-1 assay (B). Data are mean ± SD values from three independent experiments. $^{*}P < 0.05$, $^{**}P < 0.01$ and $^{***}P < 0.001$, versus vehicle control.

2.4. Cytotoxicity and growth inhibition assay

PC3 cells were plated at 3.0×10^3 cells per well in 96-well plates. Twenty-four hours after plating, increasing concentrations of KuJ were added. The cells were then incubated for 24 and 48 h at 37 °C. Cells cultures were observed microscopically and overall cell number/viability was assessed by WST-1 colorimetric assay (Roche Diagnostics, Mannheim, Germany) (Hamasaki et al., 1996). In each experiment, determinations were carried out in triplicate.

2.5. Cell cycle analysis

The cells were treated with increasing concentrations of KuJ for 24 or 48 h, then suspensions were prepared and stained with propidium iodide (Guava® cell cycle reagent, Guava Technologies, Hayward, CA, USA) according to the Guava® Cell Cycle Assay protocol. Cell cycle phase distributions were determined on a Guava® PCA Instrument using CytoSoft Software.

2.6. Apoptosis assays

Apoptosis was assessed using the Guava® Nexin reagent and the Guava® PCA system (Guava Technologies). The Guava® Nexin assay utilizes two stains (annexin V and 7-amino actinomycin D [7-AAD]) to quantitate the percentage of apoptotic cells. It was performed according to the manufacturer's protocol. After treatment with KuJ for 24 or 48 h, cell suspensions were prepared and stained with Guava® Nexin reagent for 20 min and immediately processed with the Guava PCA system. Cells were gated based on forward scatter (size), and results reported as the percentage of gated cells positive for both annexin V and 7-AAD.

2.7. Immunoblot analyses

After treatment, cells were washed twice with ice-cold phosphate buffered saline (PBS), scraped with a cell scraper into ice-cold PBS and centrifuged at 1500 rpm for 10 min. The supernatant was removed and the cell pellets were lysed with RIPA buffer (Pierce Biotechnology, Rockford, Illinois, USA) containing protease inhibitors (Pierce Biotechnology) for 15 min on ice. The insoluble matter was removed by centrifugation at 12,000 rpm for 20 min at 4 °C and supernatants were collected. Protein concentrations were determined with a Coomassie Plus™-The Better Bradford Assay Kit (Pierce Biotechnology).

Samples were mixed with 2× sample buffer (Bio-Rad Laboratories, Hercules, California USA) and heated for 5 min at 95 °C and then subjected to 10% SDS–PAGE. The separated proteins were transferred onto nitrocellulose membranes followed by blocking with 5% nonfat milk powder (w/v) in 1× TBS [10 mmol/L Tris–HCl (pH7.5), 100 mmol/L NaCl, 0.1% Tween-20] for 1 h at room temperature. Membranes were probed with antibodies for cyclin D1, cyclin E, proliferating cell nuclear

antigen (PCNA) (Santa Cruz Biotechnology, Inc., Santa Cruz, CA, USA), CDK2, CDK4 (BD Biosciences, San Jose, CA, USA), caspase-3, cleaved caspase-3, poly(ADP-ribose) polymerase (PARP), and survivin (Cell Signaling, Technology Inc., Danvers, Massachusetts, USA) in 5% nonfat dry milk, 1× TBS, 0.1% Tween-20 at 4 °C overnight. Membranes were then exposed to peroxidase-conjugated appropriate secondary antibodies and antibody binding was visualized with an enhanced chemiluminescence detection system (GE Healthcare Bio-sciences, Buckinghamshire, NA, UK). To confirm equal protein loading, each membrane was stripped and reprobed with anti-β-actin (Sigma–Aldrich, Co., St. Louis, MO, USA).

2.8. Invasion and migration assays

For the invasion and migration assays, the cells were seeded in BD Biocoat™ Matrigel™ invasion chambers and the BD Falcon 24-multiwell insert system (BD Biosciences, Qume Drive San Jose, California USA), respectively, and treated with KuJ (0, 10, 15 and 20 μM) for 12 h and 24 h. Ten microgram per milliliter fibronectin was used as a chemoattractant. Invading or migrating cells were fixed with 100% ethanol for 5 min, then stained with 0.5% crystal violet in 20% methanol for 30 min. The% areas occupied with cells were then determined with ImageJ 1.410 (National Institute of Mental Health, Maryland, USA).

2.9. Zymography

PC3 cells were maintained in serum free RPMI for 12 h then incubated with increasing concentrations of KuJ (0, 10, 15 and 20 μM) for 24 h in serum free RPMI. Matrix metalloproteinase (MMP)-2 and MMP-9 secretion into the conditioned medium was detected by gelatin zymography as previously described (Welch et al., 1990). Samples were subjected to sodium dodecyl sulfate–polyacrylamide gel electrophoresis (SDS–PAGE) using a 10% acrylamide gel containing 0.1 mg/mL of gelatin (Bio-Rad Laboratories, Hercules, California USA) under non-reducing conditions. After electrophoresis, the gel was washed twice with 2.5% Triton-X 100 then incubated at 37 °C in incubating buffer (50 mmol/L Tris–HCl, 200 mmol/L NaCl, and 10 mmol/L $CaCl_2$, pH 7.4) for 24 h. After incubation, the gel was stained with 0.1% Coomassie brilliant blue R250 (Bio-Rad Laboratories) in 50% methanol/10% acetic acid, and destained with 10% acetic acid/50% methanol. Bands of gelatinolytic activity were analyzed using ImageJ 1.410.

Urokinase plasminogen activator (uPA) secretion from PC3 cells into the culture medium was also examined by casein–plasminogen zymography (Law et al., 2005). The culture supernatant was separated by electrophoresis in a 10% polyacrylamide gel (PAGE) which was copolymerized with 1 mg/mL β-casein and 10 μg/mL human plasminogen (Sigma–Aldrich, Co., St. Louis, MD, USA) in the presence of SDS under non-reducing conditions. After electrophoresis, the gel was washed twice with 2.5% Triton X 100 and incubated in incubating buffer for 18 h at 37 °C, then stained and destained as described above.

2.10. Real-time RT-PCR

After treatment with increasing concentrations of KuJ (0, 10, 15 and 20 μM), total RNA from cell lysates was extracted with an RNAeasy® Mini kit (Qiagen sciences, Maryland, USA) and one microgram of RNA was converted to cDNA with PrimeScript™ reverse transcriptase (Takara, Shiga, Japan). cDNA samples were subjected to quantitative PCR using SYBR Premix ExTaq II (Takara) in a LightCycler apparatus (Roche Diagnostics). MMP-2, MMP-9 and MT1-MMP mRNA levels were quantified using the following primers: MMP-2 forward, 5′-gtgcctattacctgaagctg-3′ and reverse 5′-gaggagtacagtcagcatct-3′; MMP-9 forward, 5′-cactgtccacccctcaga gc-3′, and reverse 5′-gccacttgtcggcgataagg-3′; MT1-MMP forward, 5′-cgctacgccatcc agggtctcaaa-3′ and reverse 5′-cggtcatcatcgggcagcacaaaa-3′. The house keeping gene, GAPDH (glyceraldehyde-3-phosphate dehydrogenase) was used as an internal control to normalize reactions.

2.11. PC3 xenograft model

After one week of acclimation, mice were divided into three groups of 10 mice each. Two million PC3 cells were mixed with 50% Matrigel (Becton, Dickinson and Company, Franklin Lakes, NJ, USA) and injected (100 μL) subcutaneously into the back area of the mice. Mice were given a diet containing 0, 1 and 5% BMLE w/w for 15 weeks. The body weights and tumor volumes of each mouse were estimated every week. Tumor volume was calculated using the following formula: 0.52 (long axis × short axis × short axis). Mice were sacrificed at experimental week 15.

At the sacrifice, primary tumors and the heart, liver, lung, kidneys, spleen, and lymph nodes were removed and fixed in 10% buffered formalin. Primary tumors were measured and tumor volume was calculated using the following formula: 0.52 (axis1 × axis2 × axis3). At least one section of each tissue and the largest section from each lobe of the lung were processed for hematoxylin and eosin (HE) staining, Ki67 immunostaining and terminal deoxy nucleotidyl transferase-mediated dUTP nick end labeling (TUNEL) assay.

2.12. Immunohistochemistry

For Ki67 immunostaining, paraffin-embedded specimens were sectioned (5 μm) and stained with Ki67 antibody (DAKO, Denmark A/S, Glostrup, Denmark) and then with anti-rabbit secondary antibody and avidin–biotin complex (Vectastatin Elite ABC kit; Vector Laboratory, Burlingame, CA), and binding sites were visualized with diamino-benzidine. The sections were then counterstained lightly with hematoxylin for microscopic examination.

2.13. TUNEL assay

Apoptotic cells were detected by TUNEL assay. The assay was performed using an In Situ Apoptosis Detection Kit from Takara (Otsu, Japan).

2.14. Statistical analysis

All *in vitro* experiments were performed at least in triplicate to confirm reproducibility. Statistical analyses were performed with mean ± S.D. values using one-way ANOVA, the Bonferroni correction and Dunnett's test. Statistical significance was concluded with $^{*}P < 0.05$, $^{**}P < 0.01$ or $^{***}P < 0.001$.

3. Results

3.1. Effects of KuJ on the growth of PC3 cells

Microscopic observation showed a decrease of PC3 cell number after KuJ treatment, but cell death was not obviously observed (Data not shown). WST-1 assay results showed that KuJ treatment reduced the growth of PC3 cells in a concentration-dependent manner at 24 and 48 h (Fig. 1B). Treatment with KuJ for 24 h slightly decreased PC3 cell number, whereas treatment for 48 h significantly decreased cell growth of the cancer cells with an IC50 of 25 μM.

3.2. KuJ caused G1 cell cycle arrest in PC3 cells

Based on the growth inhibitory effects of KuJ on PC3 cells, concentrations of 15, 20, 25, and 30 μM KuJ were selected for further *in vitro* mechanistic studies. We examined the possible inhibitory effects of KuJ on the cell cycle machinery. As shown in Fig. 2A and B, treatment of PC3 cells with KuJ for 24 and 48 h resulted in a significantly higher proportion of cells in the G1 phase of the cell cycle: 15 μM (60%, $p < 0.01$ and 59%), 20 μM (64%, $p < 0.001$ and 70%, $p < 0.01$), 25 μM (62%, $p < 0.001$ and 65%, $p < 0.05$), and 30 μM (60%, $p < 0.01$ and 64%, $p < 0.05$), compared with control values (51% and 52%). There was a concomitant reduction in the percentage of cells in S and G2-M. These data suggest that inhibition of proliferation of PC3 cells by KuJ might be associated with an induction of G1 arrest.

3.3. Induction of apoptosis by KuJ in PC3 cells

To determine whether the KuJ-induced loss of proliferative capacity of PC3 cells was associated with the induction of apoptosis, the cells were treated with KuJ as described above and the numbers of apoptotic cells were assessed. The percentage of cells in the early and late stages of apoptosis are shown in Fig. 2C and D. Treatment of KuJ for 24 h slightly but significantly induced apoptosis of PC3 cells compared to controls (Fig. 3C). Treatment of PC3 cells by 25 and 30 μM of KuJ for 48 h resulted in a significant enhancement in the number of apoptotic cells in both the early and late stages of apoptosis (Fig. 2D): control (1% and 1%), 25 μM (14%, $P < 0.001$ and 7%, $P < 0.001$) and 30 μM (13%, $P < 0.001$ and 11%, $P < 0.001$).

3.4. Alteration of cell cycle- and apoptosis-related protein levels by KuJ

The expression of G1 positive regulators (cyclin D1, cyclin E, Cdk2, Cdk4 and PCNA) was down-regulated in a concentration-